NASA TECHNICAL MEMORANDUM

NASA TM X- 73,199

NASA TM X- 73,199

ANALYSIS OF TURBOFAN PROPULSION SYSTEM WEIGHT AND DIMENSIONS

Mark H. Waters and Edward T. Schairer

Ames Research Center
Moffett Field, California 94035

January 1977

1. Report No.	2. Government Accession No.	3. Recipient's Catalog No.
NASA TM X-73,199		

4. Title and Subtitle	5. Report Date
ANALYSIS OF TURBOFAN PROPULSION SYSTEM WEIGHT AND DIMENSIONS	6. Performing Organization Code

7. Author(s)	8. Performing Organization Report No
Mark H. Waters and Edward T. Schairer	A-6890
	10. Work Unit No. 791-40-03
9. Performing Organization Name and Address	11. Contract or Grant No
Ames Research Center Moffett Field, Calif. 94035	
	13. Type of Report and Period Covered
12. Sponsoring Agency Name and Address	Technical Memorandum
National Aeronautics and Space Administration Washington, D.C. 20546	14. Sponsoring Agency Code

15. Supplementary Notes

16. Abstract

An important factor often overlooked in aircraft preliminary design studies is the tradeoff that exists in propulsion system weight and size. This is an even more important factor when there is an emphasis on reduced aircraft noise. Engines designed specifically for low noise may have significant penalties in propulsion system weight and size. The objective of this paper is to summarize weight and dimensional relationships that can be used in aircraft preliminary design studies. These relationships must be relatively simple to prove useful to the preliminary designer, but they must be sufficiently detailed to provide meaningful design tradeoffs. All weight and dimensional relationships will be developed from data bases of existing and conceptual turbofan engines. The total propulsion system will be considered including both engine and nacelle, and all estimating relations will stem from physical principles, not statistical correlations.

17. Key Words (Suggested by Author(s))	18. Distribution Statement
Propulsion weight Turbine engines Transport aircraft	Unlimited STAR Category - 07

19. Security Classif. (of this report)	20. Security Classif. (of this page)	21. No. of Pages	22. Price*
Unclassified	Unclassified	65	$4.25

*For sale by the National Technical Information Service, Springfield, Virginia 22161

SYMBOLS

A	area, m^2 (ft^2)
B	bypass ratio
C_p	specific heat at constant pressure, $\frac{\text{joules}}{\text{kg } °K}\left(\frac{\text{BTU}}{\text{lb } °R}\right)$
D	diameter, m (ft)
f	fuel-air mass ratio
FPR	fan pressure ratio
g	acceleration of gravity, 9.9 m/sec^2 (32.2 ft/sec^2)
ΔH	enthalpy change, $\frac{\text{joules}}{\text{kg}}\left(\frac{\text{BTU}}{\text{lb}}\right)$
h	hub diameter, m (ft)
J	constant, 778 BTU/ft-lb
k	constant
L	length, m (ft)
M	Mach number
N	number; rotor speed, rpm
n	constant
OPR	overall pressure ratio
P	total pressure, N/m^2 (lb/ft^2)
T	thrust, N (lb); total temperature, °K (°R)
t	tip diameter, m (ft)
v	velocity, m/sec (ft/sec)
W	mass, kg (weight, lb)
Wa	airflow, kg/sec (lb/sec)
Wff	mass flow function, $\frac{\text{kg } °K^{1/2}}{\text{N sec}}\left(\frac{\text{lb } °R^{1/2}}{\text{lb sec}}\right)$ (see eq. (10))
γ	ratio of specific heats
Γ	see equation (A10)

λ diffuser half angle, deg

Λ turbine stage loading parameter (see eq. (A1))

η isentropic efficiency

Subscripts

C compressor, core cowl

CX core exhaust

E engine

F fan face, fan

FX fan exhaust flowpath

H hub

HPT high-pressure turbine

I inlet

LPT low-pressure turbine

SLS sea level static standard day

STG stages

T total; turbine

TIP rotor tip

Superscript

- average value

ANALYSIS OF TURBOFAN PROPULSION SYSTEM WEIGHT AND DIMENSIONS

Mark H. Waters and Edward T. Schairer

Ames Research Center

SUMMARY

An important factor often overlooked in aircraft preliminary design studies is the tradeoff that exists in propulsion system weight and size. This is an even more important factor when there is an emphasis on reduced aircraft noise. Engines designed specifically for low noise may have significant penalties in propulsion system weight and size. The objective of this paper is to summarize weight and dimensional relationships that can be used in aircraft preliminary design studies. These relationships must be relatively simple to prove useful to the preliminary designer, but they must be sufficiently detailed to provide meaningful design tradeoffs. All weight and dimensional relationships will be developed from data bases of existing and conceptual turbofan engines. The total propulsion system will be considered including both engine and nacelle, and all estimating relations will stem from physical principles, not statistical correlations.

INTRODUCTION

There are several aspects of the cycle selection, design, and installation of the turbofan propulsion system that should be considered in the preliminary design of transport aircraft. This is particularly true if the analyst has the freedom to select the engine cycle and size rather than dealing with existing turbofans that are in production or under development.

Cruise fuel consumption and engine weight are the most obvious parameters of interest. However, the geometry of the engine — frontal area and length — is also important since it has a direct bearing on the nacelle design. Nacelle weight (including the thrust reverser) and drag (spillage, cowl, friction, and boattail) are directly influenced by the engine geometry; unfortunately, the overall propulsion system weight tradeoffs with engine fuel economy and nacelle drag are sometimes overlooked.

Recent studies of commercial air transports have frequently evaluated aircraft noise. Jet noise is best controlled by the cycle selection that reduces the core jet velocity. The alternative is a mechanical suppressor. More important for the higher bypass ratio turbofan engines is fan noise, which is controlled primarily by reducing the fan tip speed and/or installing acoustic treatment material in the inlet and fan exhaust ducting. All of these cycle and design alternatives affect both engine weight and geometry, and, in the case of acoustic splitters in the fan inlet and exhaust, engine performance. The various tradeoffs between noise, engine weight, and size are difficult to evaluate in preliminary design and are frequently overlooked.

Finally, there is an emerging understanding of the design tradeoffs between engine performance and weight and engine maintenance requirements. To reduce engine weight and size for a given thrust, there has been a long-standing effort to increase the turbine inlet temperature in turbine engines, which increases specific thrust (thrust/airflow). Short duration takeoff ratings and flat ratings to maintain takeoff thrust on hot days are commonplace in all modern turbofan engines. However, engine deterioration can be traced to the number of high temperature cycles experienced by the engine; from the standpoint of lifetime airline costs, it may be desirable to sacrifice engine peak thrust performance to reduce the number of engine removals for maintenance. Any reduction in specific thrust, of course, increases weight and size. This problem is discussed in reference 1, but in the opinion of the authors, considerably more evaluation of modern turbofan engine lifetime maintenance requirements is needed before this tradeoff can be understood and applied in preliminary design studies.

The objective of this paper is to summarize turbofan propulsion system weight and dimensional relationships that can be used in preliminary transport aircraft design studies. The type of propulsion system considered is the modern turbofan engine having axial flow compressors and installed in pod-type nacelles. The total propulsion system is considered, including both engine and nacelle. All estimating relations stem from physical principles, not statistical correlations.

DATA SOURCES

The production engines used in this study are listed in table 1, along with the pertinent weight and geometric data used for each. A study of this nature depends greatly on accurate data sources; thus, references 2-19 are noted throughout this table to identify our sources. Two conceptual engines, the Pratt and Whitney STF 477 and an undesignated General Electric engine, both recently completed in studies for NASA (refs. 20 and 21), have been included in this study. The data for these engines are also noted in table 1.

Propulsion system data from the NASA-sponsored Quiet Clean Short Haul Experimental Engine Study Program (QCSEE) have been used extensively in this study. In task 1 of the QCSEE study program, one of the contractors, Detroit Diesel Allison, Division of General Motors, developed a broad data base of candidate engine performance, weights, dimensions, noise, and costs. Table 2 lists the conceptual engines and the distinguishing cycle parameters for each. The Allison designations for the engines have been preserved. More details on these study engines can be found in reference 22.

ENGINE DRY WEIGHT

Specific Weight

The most common measure of basic engine weight (frequently referred to as dry weight) is the engine specific weight. This parameter is defined as the engine dry weight divided by the maximum rated thrust at sea-level static conditions. The obvious advantage of this parameter is its simplicity — weight is tied directly to the rated thrust of the engine. However, the engine flow passages are sized by air flow and the thermodynamics in the engine; thus, specific weight is clearly coupled to the engine cycle through the specific thrust parameter.

In addition to this connection with the cycle, specific weight tends to scale with engine size. An elementary analysis highlights this point: assume engine weight W scales with the cube of the characteristic dimension D, and thrust T scales with the square of D.

$$W = k_1 D^3 \tag{1}$$

$$T = k_2 D^2 \tag{2}$$

$$\frac{W}{T} = k_3 D = k_4 \sqrt{T} \tag{3}$$

$$\therefore \frac{(W/T)_2}{(W/T)_1} = \sqrt{T_2/T_1} \tag{4}$$

Thus, specific weight scales with the square root of rated thrust. This is commonly referred to as the "three halves" law.

A more general analysis follows:

$$W = k_1 D^n \tag{5}$$

$$T = k_2 D^2 \tag{6}$$

$$\therefore \frac{(W/T)_2}{(W/T)_1} = \left(\frac{T_2}{T_1}\right)^{(n-2)/2} \tag{7}$$

Obviously if $n = 2$, specific weight is independent of thrust.

The data in figure 1 are specific weight values for commercial turbojet engines (bypass ratio = 0). Also shown are a family of straight lines which, on the log-log plot, correspond to values of the exponent n from 2.0 to 3.0. (Note that the line for $n = 3.0$ plots very nicely through these data.) Thus, turbojets appear to follow the three-halves law closely, at least over the thrust range shown.

More recent commercial turbofan engines are plotted log-log on figure 2. These data are grouped into low bypass ratio turbofans (bypass ratio less than 2.0) and high bypass ratio (bypass ratio greater than 4.0 but less than 8.0). Although there is scatter in the data, a reduction in the scaling sensitivity with higher bypass ratio turbofans is obvious. From this it appears that the specific weight for the high bypass ratio turbofans is independent of thrust size, again over the thrust range shown.

Figure 3 is a cross plot of figure 2, which approximates the scaling exponent n with the engine bypass ratio at sea-level static conditions. The band is shown rather than a single curve, but the lower curve seems the most realistic. No extrapolation below $n = 2$ is shown, but it is conceivable that very high bypass ratio turbofans could scale to reduced specific weight in the range of thrust ratings given.

Also shown on figure 3 are values of minimum thrust for scaling purposes. It is obvious that this simple scale effect will not continue to be valid for engines of smaller and smaller sea-level thrust levels. There are many possible reasons for this trend. For example: the design of parts for small engines is affected by minimum gauge requirements of the materials; if blade weights no longer scale in proportion, then hub-tip ratio increases to keep hub stresses tolerable, thus decreasing the weight flow per unit area and increasing specific weight; accessory systems may not scale as the gas generator and thus become a larger percentage of the weight for small engines; compressor and turbine efficiencies decrease due to the boundary layer problems in small passages. For these and for other reasons, one can predict that there will be some engine scale size where the engine specific weight is a minimum.

Thus, the two curves on figures 2 and 3 form the basis of a simple model to predict and scale turbofan engine specific thrust. Assuming that the technology level of the engine is approximately the same, and the cycle does not go to bypass ratios greater than those shown, this model may be adequate for preliminary design purposes. However, for advanced concept studies, a more detailed evaluation of the engine dry weight is desirable.

Reference 23, an excellent evaluation of turbofan engine weight, demonstrates how the airflow can be used to estimate engine weight. This is quite logical since component sizes are keyed to the design point airflow. The ratio of thrust to weight is then computed using standard cycle analysis to compute specific thrust:

$$\text{Thrust/Weight} = (\text{Thrust/Airflow})/(\text{Weight/Airflow}) \qquad (8)$$

Scaling of Engine Weight With Airflow

The parametric engine data developed by Allison in the QCSEE study afford a unique opportunity to evaluate turbofan engine weight trends with airflow because there is a relatively large data sample for different cycles and thrust levels. Also, the sample is consistent in terms of the design

assumptions and weight accounting. To keep the weight estimating model versatile and yet simple enough to be usable, the turbofan dry weight is broken into three components:

Fan weight - which includes both the fan section and the low-pressure or fan turbine section. The fan section includes the fan rotor, fan housing, and forward support. The low-pressure turbine section includes the transition ducting between the high- and low-pressure turbines, low-pressure turbine rotor, low-pressure turbine case and vanes, and rear bearing support. Although none of the study engines had booster stages on the low rotor spool, these would be included with the fan system weight.

Core weight - which includes the compressor rotor, case and vanes, combustor-diffuser and burner, high-pressure turbine rotor, case and vanes.

Remaining weight - which includes the fuel system, lubrication system, ignition system, bleed air system, controls, accessory gearbox, fan gearing assembly and mounting system, and engine building items such as the constant speed drive limit, hydraulic pump, starter, generator, etc.

Each of these three categories is correlated with airflow with the intention of developing a logical way of building up an estimate of engine weight based on engineering principles.

Figure 4 correlates fan weight with the total airflow pumped through the fan. The symbols on the figure relate to the study engines tabulated in table 2. Three thrust ratings are included for each engine cycle: 35,584, 88,960, 133,440 N (8,000, 20,000, and 30,000 lb) sea-level static standard day thrust. The correlations include fan tip speed and first stage hub-tip ratio, which are both factors in the stress in the fan blade root created by centrifugal force. Also included in the correlation are the number of stages in the fan plus the low-pressure turbine. (Low-pressure booster stages would also be counted here.) Figure 4 is a log-log plot and care has been taken to plot a straight line through each set of three points. The equation for these lines is noted on the figure.

The correlation appears reasonably good over a range of airflow from 90.7 to 771 kg/sec (200 to 1700 lb/sec). Obviously, to be useful, reasonable estimates for the various factors in the correlations must be made. An appendix in this report summarizes engine design data (such as tip speeds and hub-tip ratios) which are necessary to apply the correlations developed here. Also given in the appendix are the procedures for calculating the number of compressor and turbine stages.

The correlation for the core engine weight is shown in figure 5. Here, the correlation includes only the number of stages in the compressor and high-pressure turbines. The independent parameter is core airflow, which is calculated directly from the total air flow and the bypass ratio B:

$$Wa_C = \frac{Wa_T}{1 + B} \tag{9}$$

The correlation is not as good as that for the fan weight, and obviously more geometric factors could be included to improve it. However, the correlation appears to be acceptable for the purpose of preliminary design estimating. Again, a log-log plot has been used, and the equation is noted on the figure.

The third element in the weight buildup of the total engine is the remaining weight, which is shown as a ratio with the core engine weight in figure 6. The correlation, again with core airflow, is good and graphically demonstrates the significance of the subsystem weights to the total weight. These components tend to scale very little with size and, for smaller engines, become a greater weight factor than the core engine. The difference in the two curves, one for geared fan engines and the other for nongeared engines, reflects the gearbox weight. The weight tradeoff between geared turbofan engines and nongeared turbofans, which of course require more low-pressure turbine stages, can be addressed with these correlations and is presented in the Results section.

ENGINE FRONTAL DIMENSIONS

Engine Face Diameter

A critical dimension in the engine is the diameter at the fan face. Even with low bypass turbofan engines this is the maximum diameter in the engine, and dictates much of the nacelle geometry.

Axial Mach numbers do not vary widely at the engine face; 0.45 to 0.60 is the approximate spread. Thus, the diameter can be calculated easily, knowing the airflow at sea-level static conditions and the hub-tip ratio at the face of the first stage of the fan (see appendix).

Assuming

$$\frac{Wa_F\sqrt{T_F}}{A_{flow}P_F} = 0.0698M_F\frac{1}{(1 + 0.2M_F^2)^3} = Wff_F \tag{10}$$

(in English units the constant 0.0698 becomes 0.919)

at sea-level static (P_F = 101,309 N/m^2 (2116 lb/ft^2); T_F = 288 °K (519 °R)),

$$\frac{Wa_{SLS}}{A_F} = \left[1 - \left(\frac{h}{t}\right)^2\right]\frac{P_F}{\sqrt{T_F}}(Wff_F) \tag{11}$$

e.g., at h/t = 0.38 and M_F = 0.5, Wa_{SLS}/A_F = 152.3 kg/sec/m^2 (31.2 lb/sec/ft^2). Thus, the engine face frontal area and the fan diameter are computed directly

from the airflow. This relation is shown in figure 7 with lines of constant axial Mach number and actual engine data.

Once again the hub-tip ratio becomes an important factor, and one can observe an obvious weight tradeoff in its selection. The fan weight increases with reduced h/t because of blade root stresses (figure 4). However, at smaller hub-tip ratios, the diameter of the engine is reduced, allowing a smaller nacelle size and both weight and drag reductions. This tradeoff is discussed in the Results section.

Engine Core Diameter

The diameter at the face of the engine core is not as critical a dimension as that of the fan face, but it is used later to predict the length of the transition ducting from the fan exit to the face of the core. Unfortunately, this diameter is not as predictable because of the wider variation in the hub-tip ratio at the core face and the pressure and temperature rise between the fan and the core when booster stages are added in the transition ducting. However, if one assumes that the axial Mach number at the face of the core is equal to that at the fan face, the following expression can be developed:

$$\frac{A_C}{A_F} = \frac{1 - (h/t)_F^2}{1 - (h/t)_C^2} \frac{Wa_C}{Wa_F} \sqrt{\frac{T_C}{T_F}} \frac{P_F}{P_C} \tag{12}$$

The pressure and temperature rise at the core face is due to both the fan and booster stages, if there are any. Assuming an isentropic efficiency of 86%, the following relationship can be easily computed.

$$\frac{A_C}{A_F} = \frac{1 - (h/t)_F^2}{1 - (h/t)_C^2} \frac{1}{1 + B} \frac{1}{(P_C/P_F)^{0.835}} \tag{13}$$

To use this equation, estimate the hub-tip ratios and pressure ratio between the engine face and the core face from the appendix.

Turbine Exit Diameter

The turbine exit diameter is used in the calculation of the number of turbine stages. The appendix details the calculation procedure, which is similar to that shown above except that pressure and temperature ratios must be computed across the whole engine.

For turbojets, this dimension is the maximum engine diameter and thus is a factor in determining nacelle dimensions. For low-bypass ratio turbofans having mixed flow nozzles, the fan exhaust ducting over the turbine may require a diameter larger than the fan face to avoid high subsonic internal Mach numbers. Again, nacelle dimensions will be affected. Also, the turbine exhaust diameter is used to estimate the core nozzle length that is discussed in the nacelle geometry section.

ENGINE LENGTH

The calculation of engine length becomes somewhat more complicated in high bypass ratio turbofan engines because of the need to reduce the diameters in the flow path going from the fan exit to the core. This region is often called the "gooseneck." To account for the length consistently, this paper divides the engine into four regions: fan stages (from the engine front flange to the face of the last fan stage); the gooseneck (from the face of the last fan stage to the face of the engine core); the core (from the face of the engine core to the rear flange of the high-pressure turbine); and the low-pressure turbine stages (from the high-pressure turbine exit to the rear flange of the engine, which includes any transition ducting between turbines). These regions are depicted in sketch (a). Note that by this definition the fan length goes to zero for a single stage fan. Including the final fan stage with the gooseneck avoids definition problems in trying to account for different geometric design variations in splitting the flow into the core.

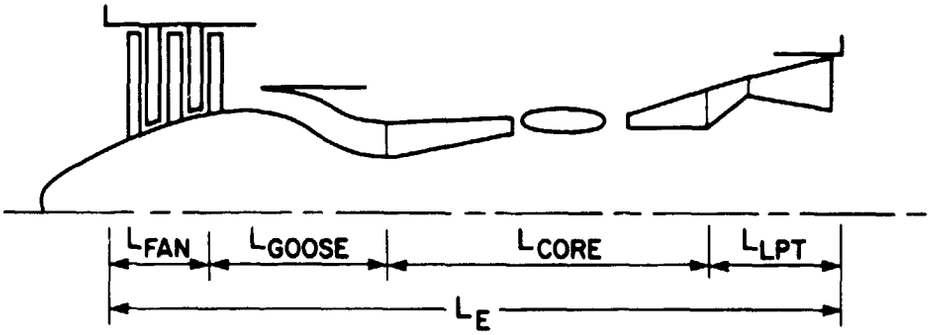

Sketch (a)

Both the inlet and nozzle are considered in a later discussion of nacelle length.

Fan Length

In estimating the length of a multistage fan, the length per stage is considered. The first stages of several turbojet engine compressors are also included in the data shown on figure 8. The correlation of fan (compressor) length per stage is plotted against an effective engine face flow path diameter to indicate scale size. The spread of the data in figure 8 is significant with the ratio of length to effective diameter per unit stage varying between 0.18 and 0.32. A mean value of 0.25 would give a reasonable estimate, but the increased spacing between fan stages may be a design requirement for reduced fan noise.

Gooseneck Length

The length of the gooseneck is dictated primarily by the reduction in flow path diameter from the face to the core. The necessary turning of the

flow path must be carefully contoured to avoid local separation and resulting total pressure losses. Frequently, engines are designed with fan exit guide vanes, or core booster stages located in the gooseneck. These additions may add to the length unless the flow is turned through these stages to reduce the flow path diameter.

Figure 9 is a correlation that allows the gooseneck length to be calculated once the fan face diameter and the core face diameter are known. As the core diameter increases relative to the fan diameter (as with low bypass ratio turbofans), the gooseneck length — as defined here — approaches the length of a single fan stage, as noted on the figure. However, for the high bypass ratio turbofans, where the core diameter may be as low as one-third the fan diameter, the gooseneck length becomes significant.

Two engines fall considerably outside the correlation band shown on figure 9. The study engine shown has an exit guide vane with all flow path turning after this vane; the production engine has several core booster stages in the flow path before diameter-reduction takes place. Thus, the approach taken by the engine designer can add significantly to the gooseneck length. However, there are definite minimum length limits represented by the lower side of the correlation band.

Core Engine Length

The length of the core engine correlates well with the log of the core compressor pressure ratio, as shown in figure 10. The square root of the core airflow indicates the scale size of the core. The log of the compressor pressure ratio relates the compression ratio to the number of compression stages, which has a direct bearing on the length of the core.

Note that the three-spool RB211 turbofan engine falls below the trend line in the figure. Adding a third spool improves compressor stage work in the high-pressure end of the compressor and thus reduces the number of compressor stages required. Such is the case for the RB211 engine; the effect on core engine length is reflected in figure 10.

Low-Pressure Turbine Length

The format for correlating the low-pressure turbine length is identical to that for the fan: length per stage is plotted against the effective diameter at the turbine exit. The correlation is shown on figure 11; the spread of data, which is significant, is similar to that for the fan length per stage (fig. 8). Again, a ratio of low-pressure turbine length per stage to the effective exit diameter of 0.25 is an acceptable mean value estimate.

There is some rational explanation for the data spread. The low-pressure turbine length includes any transition ducting between the exit of the high pressure turbine and the low-pressure turbine entrance. However, the addition of the transition piece is at the option of the designer, as demonstrated by sketch (b).

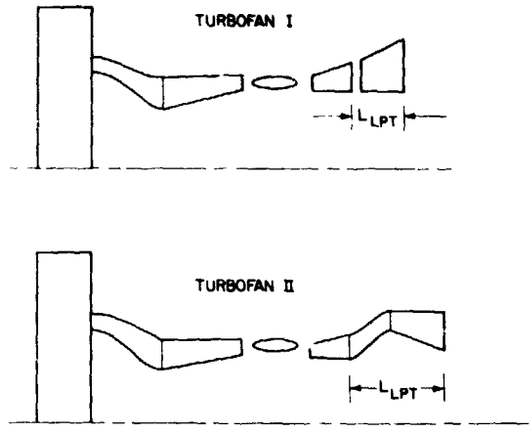

Sketch (b)

Turbofan I has no interturbine transition piece, and the low-pressure turbine is designed with a constant hub diameter and constantly increasing tip diameters. Turbofan II has a transition piece and the tip diameter of the low-pressure turbine is constant with successively reduced hub diameters. These are two extreme examples. A shorter transition piece combining increasing tip diameter and reduced hub diameter is a common design approach.

The tradeoff involved is minimum engine length versus higher turbine work per stage. Interestingly, the JT9D is an example of a Turbofan I, and the CF6 is an example of a Turbofan II. The turbine lengths plotted for these two engines in figure 11 reflect the design approach taken.

NACELLE DIMENSIONS

Calculation of the nacelle geometry is a necessary step to compute nacelle weights. In addition, nacelle geometry must be calculated to compute the external drag of the nacelle. Sketch (c) identifies the key dimensions used in this paper in defining the nacelle geometry for both short fan duct nacelles and long fan duct nacelles. To be consistent with the engine geometry already presented, the critical dimensions that lead to the geometry of the nacelle are the fan and turbine diameters and the engine length (fan face of turbine rear flange).

It is difficult to obtain consistent data to compare nacelle geometry and weights on existing production aircraft. Fortunately, a recently completed NASA study (ref. 19) has done just that; with very few exceptions, all data shown for nacelle dimensions and weights are taken from that report. These data are tabulated in table 3.

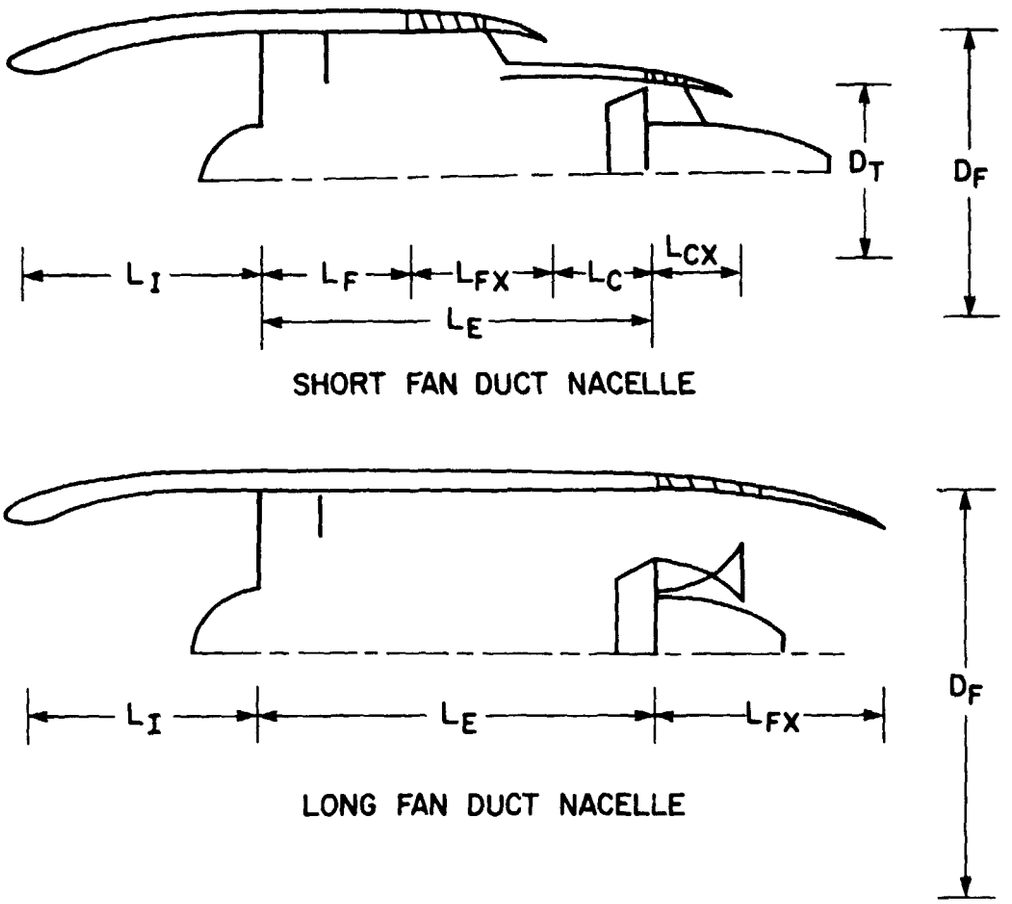

Sketch (c)

Inlet Length

It is fairly straightforward to compute the length of the inlet based on the requirement to diffuse the engine airflow from the velocity at the inlet throat to the face of the engine. However, this is a critical region for the addition of acoustic treatment, and in the future, nacelle inlets may be dictated more by this requirement than by airflow diffusion.

The sketch (d) defines the factors needed to compute the inlet length.

At takeoff, the inlet throat is typically sized for a local Mach number of 0.65 to 0.70. At the face of the engine, the Mach number is nominally 0.50 (see fig. 7). However, for proper diffusion to minimize the combined effects of flow separation and wall friction, the effective diffusion cone angle should be approximately 7°. Thus, once the engine face hub-tip ratio is

specified (typically 0.36 to 0.40 — see appendix) then the ratio of length to diameter can be computed directly.

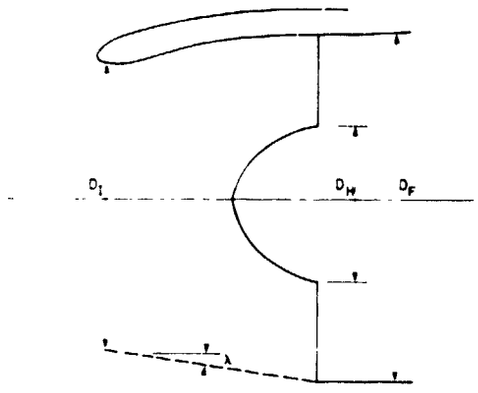

Sketch (d)

$\frac{Wa\sqrt{T}}{AP} = Wff$, as defined previously with $\gamma = 1.4$

$$\frac{h}{t} = \frac{D_H}{D_F}$$

From continuity,

$$\frac{A_I}{A_F} = \frac{Wff_F}{Wff_I}\left[1 - \left(\frac{h}{t}\right)^2\right] \tag{14}$$

From geometry

$$\frac{A_I}{A_F} = \left(1 - 2\,\frac{L_I}{D_F}\tan\lambda\right)^2 \tag{15}$$

Thus,

$$\frac{L_I}{D_F} = \frac{1 - \left\{(Wff_F/Wff_I)[1 - (h/t)^2]\right\}^{1/2}}{2\tan\lambda} \tag{16}$$

For a typical case, assume

$M_I = 0.68$, $Wff_I = 0.036$ kg $°K^{1/2}$/N sec (0.48 lb $°R^{1/2}$/lb sec)

$M_F = 0.475$, $Wff_F = 0.029$ kg $°K^{1/2}$/N sec (0.38 lb $°R^{1/2}$/lb sec)

$$\frac{h}{t} = 0.38$$

$$\lambda = 7°$$

Then,

$$\frac{L_I}{D_F} = 0.721$$

The data in figure 12 represent current nacelle designs. Since the parameters in the equation above can be juggled to change the inlet length to diameter ratio, and the spread of data is not surprising. As mentioned previously, longer inlets are usually designed to reduce fan noise.

Fan Cowl Length

The fan cowl, by definition here, includes the portion of the nacelle that wraps around the fan and fan exhaust ducting ahead of the fan nozzle and thrust reverser. This definition is limited to the short fan duct nacelle only. For the long duct nacelle, the length of the engine defines this portion of the nacelle (see sketch (c)).

The data in figure 13 relate the fan cowl length to the engine length. Note that the data group near a length-to-length ratio of 0.4. It is apparent that the design objective for the short duct nacelle is to enclose the fan flow to a point ahead of the maximum core diameter at the turbine. The thrust reverser-nozzle system then must extend far enough back to allow the fan flow to expand over the boattail of the core nozzle.

Fan Thrust Reverser and Exhaust Nozzle Length

Whereas the fan nacelle length is relatively predictable, the length of the fan thrust reverser is not, because the designer has some option in contouring the core boattail, as shown by the two examples in sketch (e).

Thus, the length L_{FX} is not very predictable, as demonstrated in figure 14. For the short fan duct nacelle, the ratio of the fan exhaust length to the fan diameter varies from <0.4 to >0.7. However, picking a nominal value such as 0.55 does not necessarily lead to unacceptable weight estimates, since the core cowl length L_C is computed as

$$L_C = L_E - (L_F + L_{FX}) \tag{17}$$

Thus, a short estimate for the length L_{FX} gives a long estimate for the length L_C and affects the nacelle weight estimate accordingly (see next section).

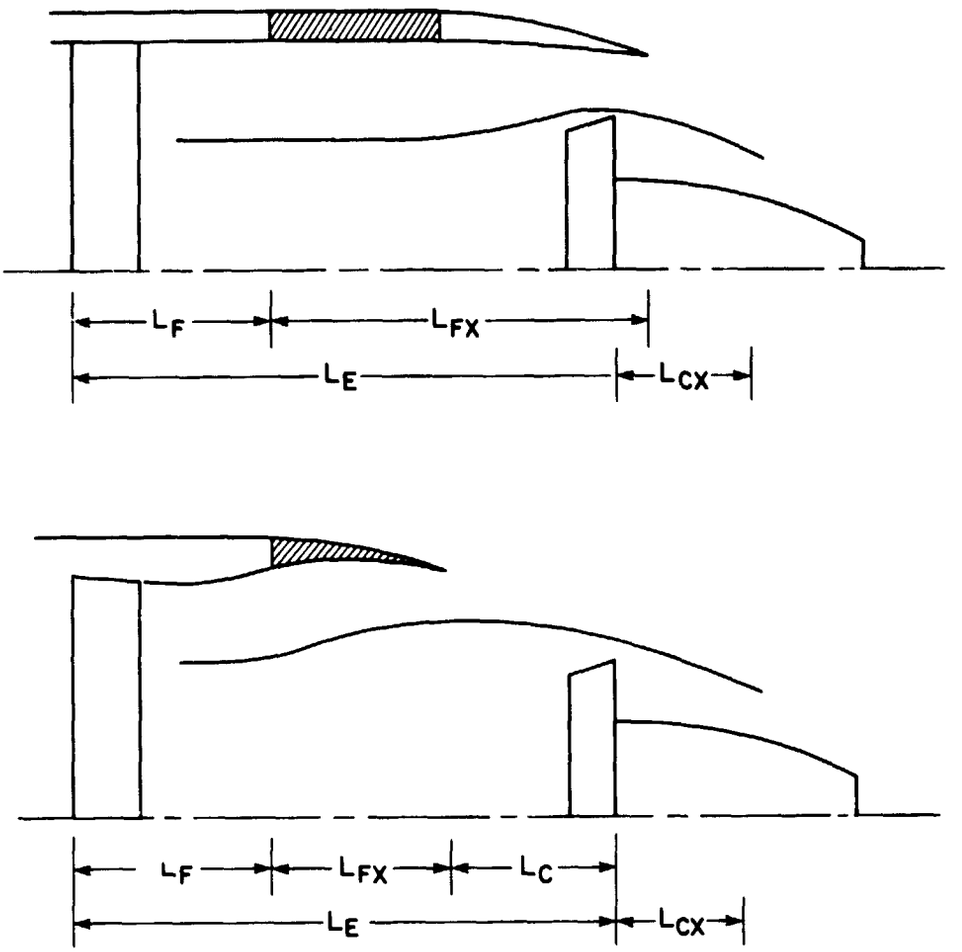

Sketch (e)

Data on figure 14 are also shown for the fan exhaust nozzle and thrust reverser on long duct nacelles. In reality, this is a mixed flow nozzle, and the ratio of the length to the diameter is longer to accommodate the mixing of the fan and core flows ahead of the nozzle.

Core Thrust Reverser and Exhaust Nozzle Length

The final element in the buildup of the total nacelle length is the core engine thrust reverser and exhaust nozzle. The data in figure 15 relate the length of the core exhaust system to the diameter at the turbine exit. Although the amount of data is again limited, it appears that the length to diameter ratio is nominally 0.9 for an exhaust system having a core flow thrust reverser and 0.5 for one without a thrust reverser.

NACELLE WEIGHTS

To account for total nacelle weight, the nacelle is subdivided into the cowling, fan exhaust system, and core exhaust system. Thus, the cowling includes the inlet cowl surface, the cowl surface covering the fan and fan exhaust ducting ahead of the fan nozzle and thrust reverser, and the exposed core cowl surface from the plane of the fan nozzle exit to the attach point for the core nozzle and thrust reverser.

Surface area is used to correlate weight, and, rather than introduce the complexity of the actual nonaxisymmetric shape of the nacelle, simple cylinders are assumed, using the fan diameter, the turbine diameter, and the lengths from the previous section.

$$A_{surface\text{-}cowl} = (L_I + L_F)\pi D_F + L_C \pi D_T \tag{18}$$

Cowl weight data are given in figure 16; a unit weight of 17.1 to 19.6 kg/m^2 (3.5 to 4.0 lb/ft^2) appears reasonable.

Similarly, the exhaust system weights can be estimated from surface area calculations. The lengths from the previous section are used, along with the fan and turbine diameters for the fan and core exhaust systems, respectively. The data are given in figure 17, a unit weight of 73.2 kg/m^2 (15 lb/ft^2) is a representative value for estimation purposes.

RESULTS

This section demonstrates how the correlations that have been developed can be used in a model to estimate weights and the relative effect on nacelle drag. The model has deficiencies, and they are highlighted in the following discussion.

Since airflow is the primary factor affecting engine weights with the correlations developed, a necessary step is the calculation of specific thrust (thrust/airflow) at sea-level static standard day conditions. The following list of cycles used in this section also lists the specific thrust for each.

Cycle	Bypass ratio	Fan pressure ratio	Overall pressure ratio	Turbine inlet, temp, °K (°R)	Specific thrust
1	5.9	1.56	24.2	1563 (2813)	30.6
2	7.5	1.32	24.2	1563 (2813)	26.5
3	9.0	1.20	24.2	1563 (2813)	22.8
4	2.8	⌣.0	24.2	1563 (2813)	38.2
5	3.2	2.5	24.2	1563 (2813)	39.1
6	4.3	2.0	24.2	1563 (2813)	35.2
7	5.0	1.75	24.2	1563 (2813)	33.4

Cycle 1 in the above table is the cycle for the General Electric CF6-6 turbofan engine. This cycle, along with the flow-path geometry and Mach numbers and fan and turbine tipspeeds of the CF6, was used as a calibration point for a computer program that calculates engine and nacelle weights, geometry, and nacelle drag.

Figure 18 shows how this program estimates specific weight over a range of rated thrust from 44,480 to 222,400 N (10,000 to 50,000 lb). The CF6 calibration point is noted and each of the three cycles[1] shown scale similarly, increasing slightly with increased thrust rating. Based on the experience with existing turbofan engines, it was anticipated that the low bypass ratio cycle engine would scale more strongly with size (see the first part of the section on Engine Dry Weight). Since this did not result, one must suspect that the model is deficient in predicting the weight of low bypass ratio turbofans. The probable source of error is the scaling of core weight with airflow (fig. 5).

Also note in figure 18 that two curves are shown for the high bypass ratio (9) engine. One curve used a turbine work factor limit of 2.0 (see appendix) and an unusually large number of low pressure stages was computed (15). The second curve is the result of increasing the turbine work factor to 3.5.[2] This reduced the number of low-pressure turbine stages to nine, a more reasonable, but still high, number.

An alternative to many low-pressure turbine stages is a gearbox between the fan the low-pressure turbine. As a rule of thumb, turbofan engines with a a cycle having a bypass ratio of 9 or greater should be geared to avoid weight penalties due to an excessive number of turbine stages. Since the remaining engine weight (fig. 6) reflects engines with and without a gearbox, the engine weight model was used to test this rule of thumb. The results, shown on figure 19, indicate that the weight tradeoff becomes favorable for a geared fan at a bypass ratio much lower than 9.0. Note that several different conditions for the bypass 9.0 nongeared engine are shown: (1) fan tipspeed held constant at the CF6 value (437 m/sec (1436 fps)), (2) tipspeed according to figure 22 (271 m/sec (890 fps)), (3) low-pressure turbine work factor increased from 2.0 to 3.5 (maximum). The cycles are noted by number on the figure. The number of fan stages and low-pressure turbine stages for each are as follows:

---

[1]The CF6 fan and turbine hub-tip ratios and Mach numbers and turbine work factor were held constant for each cycle. However, fan tipspeed varied with fan pressure ratio, as shown on figure 22 in the appendix.

[2]This high work factor would lead to very high swirl in the flow at the turbine discharge. A fixed stage of stators ("half stage") would probably be required to straighten out the flow. This has not been considered in the weight comparisons.

Cycle	Fan stages (geared and nongeared)	LPT stages	
		Nongeared	Geared
1	1	5	3
2	1	6	2
3	1	6	2
4	3	3	4
5	2	3	3
6	2	4	3
7	2	4	3
3'	1	15	
3"	1	9	

The CF6 calibration point is once again noted and the disturbing result is that the geared engine weight appears to be estimated too low. It should be pointed out that the engine data base from which these correlations were developed have no geared engines with a bypass ratio less than 9.0. With high bypass ratio engines, the gearbox is housed in the cavity inside the fan hub and gooseneck, with no apparent penalties to frame or bearing design. As the bypass ratio is reduced, this may not be the case, and weight penalties may result due to special installations for the gearbox. In any event, the geared turbofan engine weights predicted by the computer model are suspect.

The nacelle weight and cruise drag are shown on figures 20 and 21, respectively. These data are consistent with the nongeared engines of figure 19 (cycle 3 for bypass ratio 9.0). A well-defined break occurs in figure 19 where the number of fan stages changes. These breakpoints show up in the nacelle weight and drag curves as well, although smoother curves have been faired. In general, as the bypass ratio increases, cowl weight increases slightly and there is a marked tradeoff between the weight of the fan exhaust system and the core exhaust system. The net result is a modest increase in nacelle weight with higher bypass ratio and a rather significant increase in nacelle cruise drag.

CONCLUDING REMARKS

The objective of this study was to present a methodology that is reasonably detailed in the prediction of propulsion system weights and dimensions. The type of propulsion addressed is limited to subsonic turbofan engines installed in pod-type nacelles. Although detailed, the methodology is general enough to provide the proper weight and dimension trends with different turbofan cycles without resorting to detailed layouts of the engine flowpath.

In the opinion of the authors, this objective can be met, but the methodology presented here falls short of doing so. One obvious shortcoming in retrospect is the over-reliance on factors that affect blade stress when correlating fan and low-pressure turbine weight. This approach addresses

the blades, disks, and hub of the rotating machinery, but ignores the fact that the component weight also includes stators, frames, shafts, and bearings. Thus, a more accurate model may have to distinguish between rotating and non-rotating elements of each component to estimate weight properly. In addition, it may be necessary to distinguish between the fan and the low-pressure turbine and not treat the two as one component when correlating weight. With the correlation presented in this paper, a turbine stage is equated equally with a fan stage. This certainly is not true for high bypass ratio engines, which have very large fans with respect to any other component in the engine.

APPENDIX

This appendix summarizes turbofan engine design data needed to compute the correlation factors for fan weight, core weight, and several dimensional parameters. Data for both production engines and several of the QCSEE study engines are used, as noted in the tables.

Table 4 presents diameters, hub-tip ratios, and tipspeeds for the fan face, high-pressure turbine face, and low-pressure turbine exit. These data were gleaned from a variety of sources and in some cases were approximated from available engine layouts. The face hub-tip ratio is used directly in the correlation for fan weight, and a value of 0.4 to 0.45 is a representative value. Fan tipspeed is also used directly in the fan weight correlation, and figure 22 shows how this parameter tends to vary with fan stage loading (pressure ratio). A clear distinction bewteen single stage and multistage fans is evident. The only exception in the trends is the relatively high tipspeed shown for the single stage fan JT15D, which is a much smaller engine than all others listed in this appendix.

Table 5 shows pressure ratios and numbers of stages for both fans and compressors. This in turn leads to a calculation of pressure rise per stage, which is also shown. In the compressor, a pressure rise per stage of 1.2 is representative of current turbofan engine compressor design.

Tables 6 and 7 show the parameters used in computing average stage loading for the high-pressure and low-pressure turbines, respectively, and table 8 shows parameters used to compute the low-pressure turbine exit Mach number. An estimate of average stage loading is a necessary step in computing the number of turbine stages.

Calculation of the Number of HPT Stages

The calculation of the number of high-pressure turbine stages is straightforward, assuming the tipspeeds and hub-tip ratios are known. From table 6, values of 427 m/sec (1400 ft/sec) and 0.86, respectively, are representative. A rule of thumb that applies well for high-pressure turbines is that the average stage-loading parameter should not exceed a value of 2. Thus,[3]

$$\frac{\Delta H_{HPT}}{\bar{v}^2 N_{STG}} = \Lambda \leq 2.0 \tag{A1}$$

$$N_{STG} = \frac{\Delta H_{HPT}}{\bar{v}^2_{HPT}} \times \frac{1}{\Lambda_{HPT}} \tag{A2}$$

With $\Lambda = 2.0$, round this calculation to the next highest integer, e.g., $N_{STG} = 1.2 \rightarrow N_{STG} = 2$. Note that

[3]In English units multiply ΔH_{HPT}(BTU/lb) by gJ = 32.2 × 778.

$$\Delta H_{HPT} = \frac{\Delta H_{HPC}}{1 + f} \tag{A3}$$

$$V_{HPT} = \frac{V_{TIP} + V_{HUB}}{2} = \frac{V_{TIP_{HPT}}(1 + h/t_{HPT})}{2} \tag{A4}$$

Calculation of Number of LPT Stages

The calculation of the low-pressure turbine stages is somewhat more complicated for nongeared turbofan engines because the tipspeed of the fan governs the tipspeeds in the LPT. Again, the average stage loading parameter Λ is assumed and frequently is greater than 2.0 (table 7).

$$N_{STG_{LPT}} = \frac{\Delta H_{LPT}}{\bar{v}^2_{LPT}} \times \frac{1}{\Lambda_{LPT}} \tag{A5}$$

With

$$\Delta H_{LPT} = \Delta H_F \frac{1 + B}{1 + f} \tag{A6}$$

$$\bar{v}_{LPT} = V_{TIP_{LPT}} \frac{1 + h/t_{LPT}}{2} \tag{A7}$$

It is the calculation of $V_{TIP_{LPT}}$ that adds to the complexity

$$V_{TIP_{LPT}} = V_{TIP_F} \frac{D_{LPT}}{D_F} = V_{TIP_F} \sqrt{\frac{A_{LPT}}{A_F}} \tag{A8}$$

$$\frac{A_{LPT}}{A_F} = \frac{Wff_F}{Wff_{LPT}} \frac{1}{\Gamma} \frac{1}{1} \frac{+ f}{+ B} \frac{1 - (h/t)^2_F}{1 - (h/t)^2_{LPT}} \tag{A9}$$

for

$M_F = 0.5$, $Wff_F = 0.030$ kg $°K^{1/2}$/N sec (0.39 lb $°R^{1/2}$/lb sec) ($\gamma = 1.4$)

for

$M_{LPT} = 0.4$, $Wff_{LPT} = 0.026$ kg $°K^{1/2}$/N sec (0.335 lb $°R^{1/2}$/lb sec) ($\gamma = 1.35$)

$$\Gamma \equiv \frac{(P/\sqrt{T})_{LPT}}{(P/\sqrt{T})_F} \tag{A10}$$

For clarification use the following stations:

1 fan face

4 high-pressure turbine inlet

6 low-pressure turbine exit

$$\Gamma = \frac{P_6}{P_1}\sqrt{\frac{T_1}{T_6}} = \frac{P_6}{P_4}\frac{P_4}{P_1}\sqrt{\frac{T_1}{T_4}\frac{T_4}{T_6}} \tag{A11}$$

Turbine inlet temperature T_4 and the overall pressure ratio OPR are specified for the engine. Thus, $T_4/T_1 = T_4(°K)/288$; $P_4/P_1 = 0.96$ OPR (accounts for combustor pressure drop).

$$\frac{T_4}{T_1} = \frac{T_4(°K)}{288}$$

$$\frac{P_4}{P_1} = 0.96 \text{ OPR (accounts for combustor pressure drop)}$$

$$\frac{T_6}{T_4} = 1 - \frac{(1/\eta_C)(OPR^{0.27} - 1) + (B/\eta_F)(FPR^{0.286} - 1)}{(1 + f)(T_4/T_1)\eta_T(\bar{C}_{P_T}/\bar{C}_{P_C})} \tag{A12}$$

typical value of $\bar{C}_{P_T}/\bar{C}_{P_C} = 1130/1005 = 1.12$ $(0.27/0.24 = 1.12)$

$$\frac{P_6}{P_4} = f\left(\frac{T_6}{T_4}, \eta_T, T_4\right)$$

This parameter cannot be calculated in a simple closed form without introducing a significant error due to the changing gas properties during the turbine expansion. The series of curves in figure 23 represent this function for $\eta_T = 0.90$. The hub-tip ratios can be estimated from tables 6 and 7.

$$\left(\frac{h}{t}\right)_F \approx 0.4 - 0.45$$

$$\left(\frac{h}{t}\right)_{LPT} \approx 0.55 - 0.60$$

Although this calculation appears formidable, it lends itself to a simple computer program. Obviously, the problems arise from selecting the proper geometric inputs.

For geared fans, the calculations of LPT stages revert to the simpler form for the HPT since LP turbine tipspeed can be set independently from the fan tipspeed. Note the higher LPT tipspeeds for the geared fan engines listed in table 6.

REFERENCES

1. Swan, W. C.; Bouwer, D. W.; and Tolle, F. F.: Life Cycle Cost Impact on Design Considerations for Civil Transport Aircraft Propulsion Systems. Third International Symposium on Air Breathing Engines, Munich, Germany, March 7-12, 1976.

2. Pratt and Whitney Turbine Engine Guide. Pratt and Whitney Aircraft, November, 1975.

3. Taylor, J. W. R., ed.: Jane's All the World's Aircraft, 1975-76. Franklin Watts Inc. (New York), 1975.

4. Hague, D. S.; Vandenberg, J. D.; and Woodbury, N. W.: Multivariate Analysis, Retrieval, and Storage System (MARS). Vol. IV, Turbojet and Turbofan Data Base (By Engine). NASA CR-137674, 1974.

5. Product Information. Aircraft Engine Group, General Electric Company, August 1975.

6. Taylor, J. W. R., ed.: Jane's All the World's Aircraft, 1966-67. Franklin Watts Inc. (New York), 1966.

7. Taylor, J. W. R., ed.: Jane's All the World's Aircraft, 1967-68. Franklin Watts Inc. (New York), 1967.

8. ALF 502 Turbofan Engine. Avco Lycoming Division, Stratford, Connecticut, 1974.

9. CF6 High Bypass Turbofans. General Electric Aircraft Engine Group, Cincinnati/Lynn, 1975.

10. JT15D Commercial Turbofan: Status and Information Report. United Aircraft of Canada Limited, Longview, Quebec, 1970.

11. Thomas, W. H.: Unique Features of the TF41 Turbofan. Paper 690687, presented at SAE National Aeronautic and Space Engineering and Manufacturing Meeting, Los Angeles, Calif., Oct. 1969.

12. Fink, D. E.: M49 Larzac Testing Under Way. Aviation Week and Space Technology, Nov. 23, 1970, pp. 40-44.

13. TF34-GE-100 Installation Data. General Electric Aircraft Engine Group, Lynn, Mass., 1973.

14. Yaffee, M. L.: Lycoming Enters Turbofan Arena. Aviation Week and Space Technology, Aug. 21, 1972, pp. 44-47.

15. Yaffee, M. L.: Pratt and Whitney Builds on JT9D Concept. Aviation Week and Space Technology, June 24, 1974, pp. 49-54.

16. Keen, J. M. S.: Development of the Rolls-Royce RB.211 Turbofan for Airline Operation. Paper 700292, presented at SAE National Air Transportation Meeting, New York, N. Y., April 1970.

17. RB.211 Development Program on Schedule. American Aviation, Sept. 30, 1968, p. 32.

18. RB.401 Turbofan Engine. Rolls-Royce (1971) Limited Bristol Engine Division, Bristol, 1975.

19. Parametric Study of Transport Aircraft Systems Weight and Cost. PRC Systems Sciences Company, Report No. R-1816, 1974.

20. Gray, D. E.: Study of Unconventional Aircraft Engine Designed for Low Energy Consumption. NASA CR-135065, 1976.

21. Nietzel, R. E.; Hirsckron, R.; and Johnston, R. P.: Study of Turbofan Engines Designed for Low Energy Consumption. NASA CR-135053, 1976.

22. Helms, H. E.: Quiet Clean STOL Experimental Engine Study Program, Task I - Parametric Propulsion System Studies. NAS3-16727, 1972.

23. Gerend, Robert P.; and Roundhill, John P.: Correlation of Gas Turbine Engine Weights and Dimensions. AIAA Paper 70-669, AIAA Sixth Propulsion Joint Specialist Conference, San Diego, Calif., June, 1970.

TABLE 1.- ENGINE DATA

Low Bypass Turbofans

	JT3D-3B	JT8D-7	JT8D-15	JT15D-1	TFE731-2	CF700-20-2	CJ805-23B	TF41-A-1	M49-01
Thrust, SLS, N (lb)	80,064 (18,000)	62,272 (14,000)	68,944 (15,500)	9,786 (2,200)	15,568 (3,500)	20,016 (4,500)	71,613 (16,100)	64,496 (14,500)	10,230 (2,300)
Airflow, SLS, kg/sec (lb/sec)	211 (465)	143 (315)	147 (324)	34 (75)	51 (113)	58 (128)	191 (422)	117 (258)	26 (57)
Bypass ratio, SLS		1.1	0.99	3.28	2.66	1.97	1.46	0.76	1.4
Dry weight, kg (lb)	1,968 (4,340)	1,453 (3,205)	1,501 (3,309)	229 (506)	322 (710)	334 (737)	1,708 (3,766)	1,440 (3,175)	260 (573)
Fan tip diam, m (in.)	1.27 (50)	1.04 (41)	1.04 (41)	0.533 (21)	0.711 (28)			0.965 (38)	0.432 (17)
Turbine tip diam, last stage, m (in.)	0.939 (37)	0.813 (32)	0.813 (32)					0.711 (28)	
Engine length, face to flange, m (in.)	3.40 (134)	2.84 (112)	2.84 (112)	1.29 (51)	1.27 (50)		3.33 (131)	2.62 (103)	1.14 (45)
Number stages									
Fan	2	2	2	1	1	1(aft)	1(aft)	3	2
LPC/HPC	6/7	4/7	4/7	1 cent	4 ax, 1 cent	8	17	2/11	4
HPT/LPT	1/3	1/3	1/3	1/2	1/3	2	3/1	2/2	1/1
References	2,4	2,3	2,3	3,10	3	5	6	3,11	12,3

TABLE 1.- ENGINE DATA - CONTINUED

Low Bypass Turbofans - Concluded

	SPEY MK512	SNECMA M53	TF30-P-408
Thrust, SLS, N (lb)	53,198 (11,960)	54,933 (12,350)	59,603 (13,400)
Airflow, SLS, kg/sec (lb/sec)		84 (185)	
Bypass ratio, SLS			
Dry weight, kg (lb)	1,167 (2,574)	1,419 (3,130)	1,180 (2,602)
Fan tip diam, m (in.)			
Turbine tip diam, last stage, m (in.)			
Engine length, face-to-flange, m (in.)		4.83 (190)	2.66 (105)
Number stages			
Fan	5	3	2
LPC/HPC	12	5	7/7
HPT/LPT	2/2	2	1/3
References	3	3	2,3

TABLE 1.- ENGINE DATA - CONTINUED

High Bypass Turbofans

	CFM56	TF34-100	CF6-6D	CF6-50	ALF502H	JT9D-7	JT9D-59	RB.211-22	RB.401-07
Thrust, SLS, N (lb)	97,856 (22,000)	40,321 (9,065)	177,920 (40,000)	217,952 (49,000)	28,912 (6,500)	213,059 (47,900)	235,744 (53,000)	186,816 (42,000)	24,019 (5,400)
Airflow, SLS, kg/sec (lb/sec)	354 (780)	151 (333)	593 (1,307)	652 (1,439)	109 (240)	653 (1,440)	743 (1,639)	626 (1,380)	
Bypass ratio, SLS	5.9	6.2	5.9	4.4	6.1	5.15	4.9	5.0	4.5
Dry weight, kg (lb)	1,882 (4,150)	647 (1,427)	3,521 (7,765)	3,789 (8,355)	565 (1,245)	3,982 (8,780)	4,145 (9,140)	2,881 (6,353)	476 (1,050)
Fan tip diam, m (in.)	1.80 (71)	1.09 (43)	2.18 (86)	2.18 (86)	1.04 (41)	2.33 (92)	2.39 (94)	2.18 (86)	
Turbine tip diam, last stage, m (in.)		0.68 (27)	1.22 (48)	1.22 (48)		1.35 (53)	1.37 (54)	1.27 (50)	
Engine length, face to flange, m (in.)		1.98 (78)	4.44 (175)	4.27 (168)	1.42 (56)	3.25 (128)	3.35 (132)	3.02 (119)	
Number stages									
Fan	1	1	1	1	1	1	1	1	1
LPC/HPC	3/9	14	1/16	3/14	7 axial 1 centrifugal	3/11	4/11	7/6	9
HPT/LPT	1/4	2/4	2/5	2/4	2/2	2/4	2/4	1/1/3	1/2
References	3,5	5	5,9	5,9	3,8,14	2,3,4	2,3,15	3,16,17	3,18

TABLE 1.- ENGINE DATA - CONTINUED

High Bypass Turbofans - Concluded

	JT10D ●	STF477 ◣	G.E. Adv. Eng. ▲
Thrust, SLS, N (lb)	108,976 (24,500)	118,094 (26,550)	147,674 (33,200)
Airflow, SLS, kg/sec (lb/sec)			
Bypass ratio, SLS	5.35		7.5
Dry weight, kg (lb)	2,177 (4,800)	1,787 (3,940)	
Fan tip diam, m (in.)		1.91 (75)	2.00 (79)
Turbine tip diam, last stage, m (in.)		1.02 (40)	1.04 (41)
Engine length, face-to-flange, m (in.)		2.87 (113)	2.59 (102)
Number stages			
Fan	1	1	1
LPC/HPC	12	3/10	3/9
HPT/LPT	2/4	2/5	1/4
References	3	19	21

TABLE 1.- ENGINE DATA - CONCLUDED

Turbojets

	CJ805-3 ●	CJ610-1 ■	CJ610-8 ◆	J52-P-6A ▲	JT12A-8 ◢	JT3C-6 ◢	JT4A-3 ●
Thrust, SLS, N (lb)	49,817 (11,200)	12,677 (2,850)	13,789 (3,100)	37,808 (8,500)	14,678 (3,300)	60,048 (13,500)	70,278 (15,800)
Airflow, SLS, kg/sec (lb/sec)	76 (168)	20 (44)	20 (44)			91 (200)	
Dry weight, kg (lb)	1,270 (2,800)	181 (399)	185 (407)	932 (2,056)	212 (468)	1,920 (4,234)	2,277 (5,020)
1st stage diam, m (in.)					0.483 (19)		
Turbine tip diam, last stage, m (in.)							
Engine length, face-to-flange, m (in.)				3.022 (119)	1.57 (62)	4.24 (167)	3.66 (144)
Number stages							
LPC/HPC	17	8	8	12	9	9/7	8/7
HPT/LPT	3	2	2		2	1/2	1/2
References	6	5	5	3	2,3	7	7

TABLE 2.- STUDY ENGINES PD287

Geared (SLS thrust = 88,960 N (20,000 lb))

	-21 ○	-22 □	-23 ◇	-24 △	-25 ◺	-26 ◺	-27 ⌂	-28 ◇	-30 ◊
Airflow, SLS, kg/sec (lb/sec)	506 (1117)	423 (933)	342 (755)	506 (1115)	507 (1118)	507 (1119)	506 (1117)	506 (1116)	498 (1099)
Bypass ratio, SLS	21.5	14.8	9.0	18.2	26.0	29.4	22.0	20.0	20.7
Dry weight, kg (lb)	1225 (2701)	1263 (2785)	1404 (3095)	1266 (2791)	1190 (2623)	1173 (2588)	1243 (2741)	1224 (2700)	1209 (2665)
Fan weight, fan + LPT, kg (lb)	744 (1641)	736 (1624)	815 (1796)	749 (1651)	741 (1634)	740 (1632)	749 (1652)	743 (1638)	724 (1596)
Core weight, comp + comb + HPT, kg (lb)	189 (417)	219 (482)	260 (573)	224 (493)	158 (349)	143 (315)	197 (435)	192 (423)	193 (426)
Remaining weight, kg (lb)	292 (643)	308 (679)	329 (726)	294 (649)	290 (640)	291 (641)	297 (654)	290 (639)	292 (643)
Fan tip diam, m (in.)	2.11 (83)	1.93 (76)	1.70 (67)	2.11 (83)	2.11 (83)	2.11 (83)	2.11 (83)	2.11 (83)	2.11 (83)
Turbine tip diam, m (in.)	0.71 (28)	0.79 (31)	0.91 (36)	0.76 (30)	0.68 (27)	0.66 (26)	0.74 (29)	0.68 (27)	0.71 (28)
Engine length, face-to-flange, m (in.)	2.69 (106)	2.72 (107)	2.69 (106)	2.95 (116)	2.74 (108)	2.69 (106)	2.84 (112)	2.72 (107)	2.64 (104)
Number stages									
Fan	1	1	1	1	1	1	1	1	1
LPC/HPC	11	11	10	11	11	11	9	11	11
HPT/LPT	2/3	2/3	2/2	2/3	2/3	2/3	2/3	2/3	2/3

TABLE 2.- STUDY ENGINES PD287 - CONCLUDED

Nongeared (SLS thrust = 88,960 N (20,000 lb))

	-42 ◇	-43 ⬠	-44 ◿	-45 ⬠	-47 ⬭	-48 ◹
Airflow, SLS, kg/sec (lb/sec)	238 (525)	222 (490)	243 (535)	234 (516)	237 (524)	239 (528)
Bypass ratio, SLS	3.5	2.8	2.9	4.2	3.6	3.3
Dry weight, kg (lb)	1522 (3356)	1645 (3627)	1571 (3464)	1473 (3247)	1572 (3468)	1501 (3310)
Fan weight, fan + LPT, kg (lb)	1009 (2225)	1117 (2464)	1009 (2226)	1004 (2214)	1030 (2272)	997 (2199)
Core weight, comp + comb + HPT, kg (lb)	303 (668)	305 (672)	351 (773)	257 (566)	326 (720)	297 (655)
Remaining weight, kg (lb)	210 (463)	222 (490)	211 (465)	212 (467)	216 (476)	207 (456)
Fan tip diam, m (in.)	1.40 (55)	1.37 (54)	1.42 (56)	1.40 (55)	1.40 (55)	1.42 (56)
Turbine tip diam, m (in.)	1.07 (42)	1.12 (44)	1.09 (43)	1.07 (42)	1.09 (43)	1.07 (42)
Engine length, face-to-flange, m (in.)	3.33 (131)	3.43 (135)	3.38 (133)	3.35 (132)	3.51 (138)	3.38 (133)
Number stages						
Fan	3	3	3	3	3	3
LPC/HPC	8	8	8	8	7	9
HPT/LPT	2/3	2/3	2/2	2/4	2/3	2/3

TABLE 3.- NACELLE DATA

	JT8D-9 (DC-9-30)	JT3D-3B (DC-8-55)	JT3D-3B (DC-8-62)	CF6-6D (DC-10-10)	JT9D-15 (DC-10-40)	RB.211-22 (L1011)	JT9D-7 (B747)	CF6-50
Dimensions								
Inlet length, m (in.)	0.711 (28)	1.17 (46)	0.91 (36)	1.50 (59)	1.80 (71)	1.24 (49)	1.22 (48)	
Fan shroud length, m (in.)	3.05 (120)	1.24 (49)	3.27 (129)	1.55 (61)	1.37 (54)	1.27 (50)	1.12 (44)	1.52 (60)
Fan thurst reverser length, m (in.)		0.89 (35)		1.17 (46)	1.57 (62)	1.65 (65)	0.86 (34)	1.24 (49)
Core cowl length, m (in.)	0 (0)	1.14 (45)	0 (0)	1.73 (68)	0.30 (12)	0.10 (4)	1.27 (50)	
Primary thrust reverser length, m (in.)	1.35 (53)	1.37 (54)	1.47 (58)	0.63 (25)	1.45 (57)		1.09 (43)	1.14 (45)
Weights								
Cowl, kg (lb)	155 (341)	218 (481)	330 (727)	509 (1124)	505 (1113)	344 (760)		
Fan thrust reverser, kg (lb)		248 (547)		607 (1338)	797 (1758)	682 (1503)		
Primary thrust reverser, kg (lb)	178 (392)	330 (728)	507 (1117)	207 (456)	390 (859)	221 (487)		
References	20	20	20	20	20	20	20	21

TABLE 4.- FAN AND TURBINE DATA

Engine	Diameters, m (in.)			Hub-to-tip			Tipspeeds, m/sec (ft/sec)		
	Fan[a]	HPT[a]	LPT[b]	Fan[a]	HPT[a]	LPT[b]	Fan[a]	HPT[a]	LPT[b]
CF6-6	2.19 (86.4)	0.86 (33.9)	1.23 (48.4)	0.38	0.86	0.58	438 (1436)	447 (1468)	245 (804)
CF6-50	2.19 (86.4)	0.86 (33.9)	1.24 (48.7)	0.38	0.86	0.60	457 (1501)	474 (1555)	258 (846)
TF34-100	1.08 (42.5)	0.48 (18.8)	0.69 (27.0)	0.42	0.89	0.71	416 (1365)	447 (1468)	258 (846)
JT9D-7	2.34 (92.3)	0.94 (37.0)	1.34 (52.6)	0.37	0.87	0.57	409 (1341)	354 (1163)	235 (772)
JT8D-15	1.04 (41.0)	0.68 (26.6)	0.81 (32.0)	0.37	0.75	0.49	452 (1484)		353 (1158)
ALF502H	1.04 (41.0)			0.42			388 (1274)		
JT15D-1	0.53 (21.0)	0.31 (12.1)	0.38 (15.0)	0.40	0.77	0.60	447 (1466)	527 (1729)	319 (1047)
TF41-A-1	0.96 (37.7)	0.56 (22)	0.69 (27)	0.37	0.86	0.53	449 (1472)	374 (1226)	326 (1068)
PD287-21	2.10 (82.8)			0.45			279 (915)		
PD287-22	1.92 (75.6)		0.79 (31.0)	0.45		0.50	316 (1040)		345 (1134)
PD287-23	1.70 (67.0)			0.45			399 (1310)		
PD287-42	1.41 (55.4)			0.45			436 (1430)		
PD287-43	1.36 (53.6)			0.45			466 (1530)		

[a]Entrance of fan and HPT
[b]Exit of LPT

TABLE 5.- FAN AND COMPRESSOR STAGE PRESSURE RATIOS

Engine	Fan			Compressor		
	FPR	Stages	PR/STG	CPR	Stages[a]	PR/STG
TF34-100	1.5	1	1.5	13.2	14	1.202
CF6-6D	1.56	1	1.56	15.51	17	1.174
CF6-50A	1.69	1	1.69	16.6	17	1.179
CF34	1.40	1	1.40	12.5	14	1.197
JT9D-7	1.6	1	1.6	13.9	14	1.206
JT15D-1	1.5	1	1.5			
ALF502H	1.45	1	1.45			
TF41-A-1	2.37	2	1.54	8.4	13	1.177
TF41-A-2	2.49	2	1.58	8.59	13	1.180
JT12A-8				6.8	9	1.237
JT8D-15	2.04	2	1.428	17.64	11	1.298

[a]Number of stages includes boost stages from fan rotor as well as compressor and high pressure compressor stages.

TABLE 6.- HIGH-PRESSURE TURBINE AVERAGE STAGE LOADING

Engine	ΔH_{HPT}, J/kg (BTU/lb)	D_{HPT}, 1st stage, m (in.)	$(h/t)_{HPT}$	N_{HPT}, (rpm)	$V_{TIP_{HPT}}$, m/sec (ft/sec)	$\bar{V}$, m/sec (ft/sec)	$N_{STG_{HPT}}$	$\frac{\Delta H}{(1 + f)\bar{V}^2 N_{STG}}$ [1]
TF34-100	427,276 (183.5)	0.48 (18.8)	0.899	17,900	477 (1468)	422 (1386)	2	1.169
CF6-6	490,378 (210.6)	0.86 (33.9)	.87	9,925	447 (1468)	418 (1372)	2	1.368
JT9D-7	449,163 (192.9)	0.94 (37.0)	.87	7,330	360 (1183)	337 (1106)	2	1.928
TF41-A-1	391,417 (168.1)	~0.55 (~22)	.86	12,770	374 (1226)	347 (1140)	2	1.587
JT15D-1	282,910 (121.5)	0.31 (12.1)	.77	32,760	527 (1729)	466 (1530)	1	1.276

[1] In English units multiply ΔH_{HPT} by $gJ = 32.2 \times 778$.

TABLE 7.- LOW-PRESSURE TURBINE AVERAGE STAGE LOADING

	ΔH_{LPT}, J/kg (BTU/lb)	$\frac{D_T}{D_F}$	$(h/t)_{LPT}$, last stage	V_{TIP_F}, m/sec (ft/sec)	V_{TIP_T}, m/sec (ft/sec)	$\bar{V}_T$, m/sec (ft/sec)	$N_{STG_{LPT}}$	$\frac{\Delta H}{(1 + f)\bar{V}^2 N_{STG}}$ [1]
TF34-100	298,278 (128.1)	0.62	0.71	416 (1365)	258 (846)	220 (723)	4	1.499
CF6-6	353,230 (151.7)	.56	.58	438 (1436)	245 (804.4)	194 (635)	5	1.848
JT9D-7	298,045 (128.0)	.576	.57	409 (1341)	235 (722)	185 (606)	4	2.133
ALF502H	264,515 (113.6)			388 (1274)				
TF41-A-1	174,775 (75.06)	.726	.53	449 (1472)	326 (1068)	249 (817.5)	2	1.378
JT15D-1	177,313 (76.15)	.714	.60	446 (1466)	319 (1047)	255 (837.4)	2	1.335
PD287-22 (GR = 2.66)		.41	.50	317 (1040)	346 (1134)	259 (850.6)	3	
PD287-42	454,286 (195.1)	.758	.517	436 (1430)	330 (1084)	251 (822.1)	3	2.34

[1] In English units multiply ΔH_{LPT} by $gJ = 32.2 \times 778$.

TABLE 8.- LOW PRESSURE TURBINE EXIT MACH NUMBER

Engine	Wa_{SLS}, kg/sec (lb/sec)	Wa_{CORE}, kg/sec (lb/sec)	T_6, °K (°R)	P_6, N/m^2 (psf)	A_6, m^2 (ft^2)	Wff_6, kg $\sqrt{°K}$/N sec (lb $\sqrt{°R}$/lb sec)	M_6
CF6-6	593 (1307)	85.9 (189.4)	894 (1609)	160,821 (3359)	0.777 (8.37)	0.0206 (0.277)	0.32
TF34-100	151 (333)	20.9 (46.25)	878 (1580)	150,917 (3152)	0.183 (1.97)	0.0224 (0.303)	0.36
JT9D-7	653 (1440)	106 (234.1)	878 (1580)	160,014 (3342)	0.921 (9.92)	0.0213 (0.287)	0.33
TF41-A-1	117 (258)	64.5 (146.6)	940 (1692)	291,445 (6087)	-0.28 (-3.02)	0.0242 (0.335)	0.40
JT15D-1	34 (75)	7.94 (17.52)	831 (1497)	158,195 (3304)	0.073 (0.785)	0.0198 (0.266)	0.31
PD287-42	238 (525.2)	52.9 (116.7)	884 (1592)	114,672 (2395)	0.654 (7.04)	0.0209 (0.283)	0.33

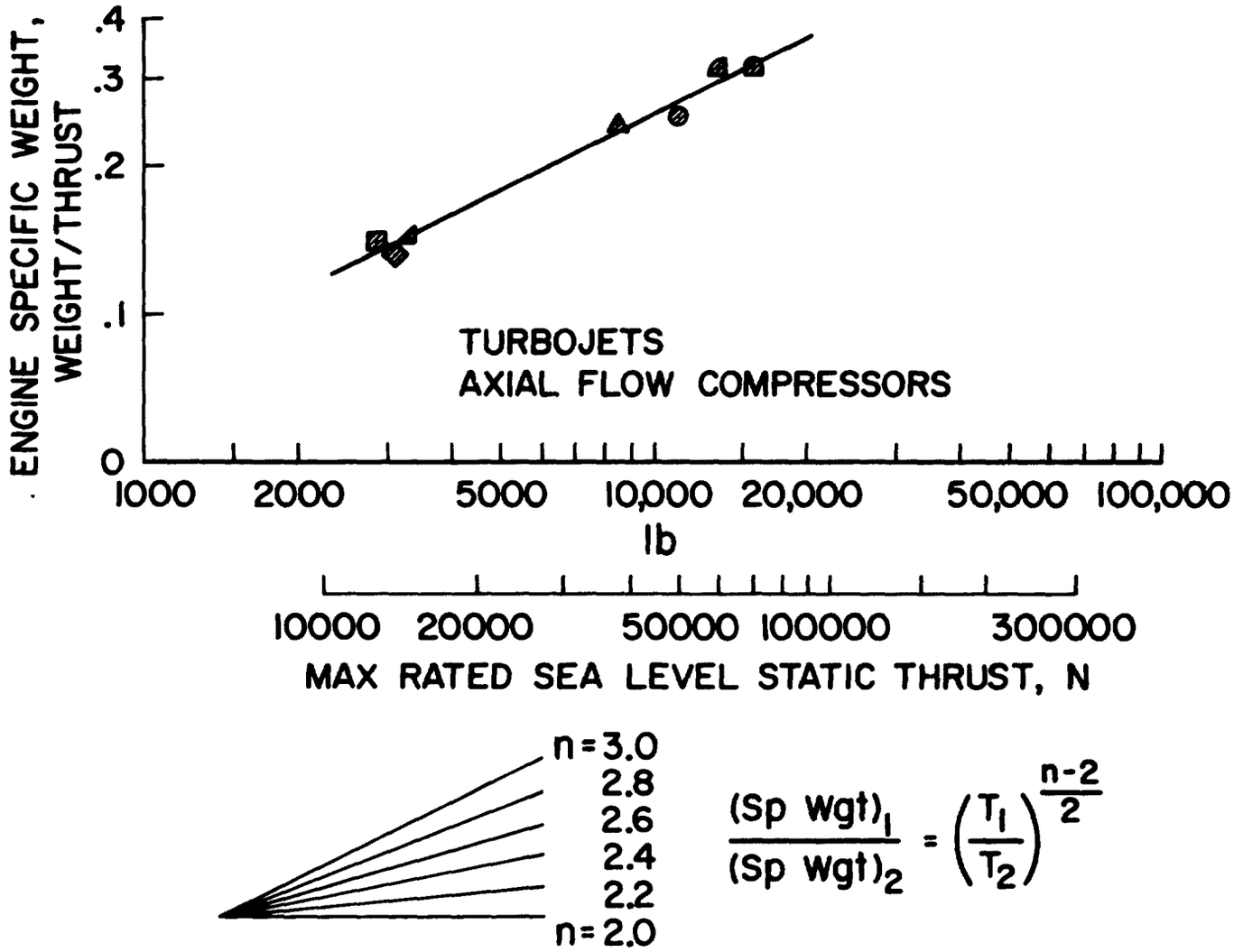

Figure 1.- Turbojet engine specific weights.

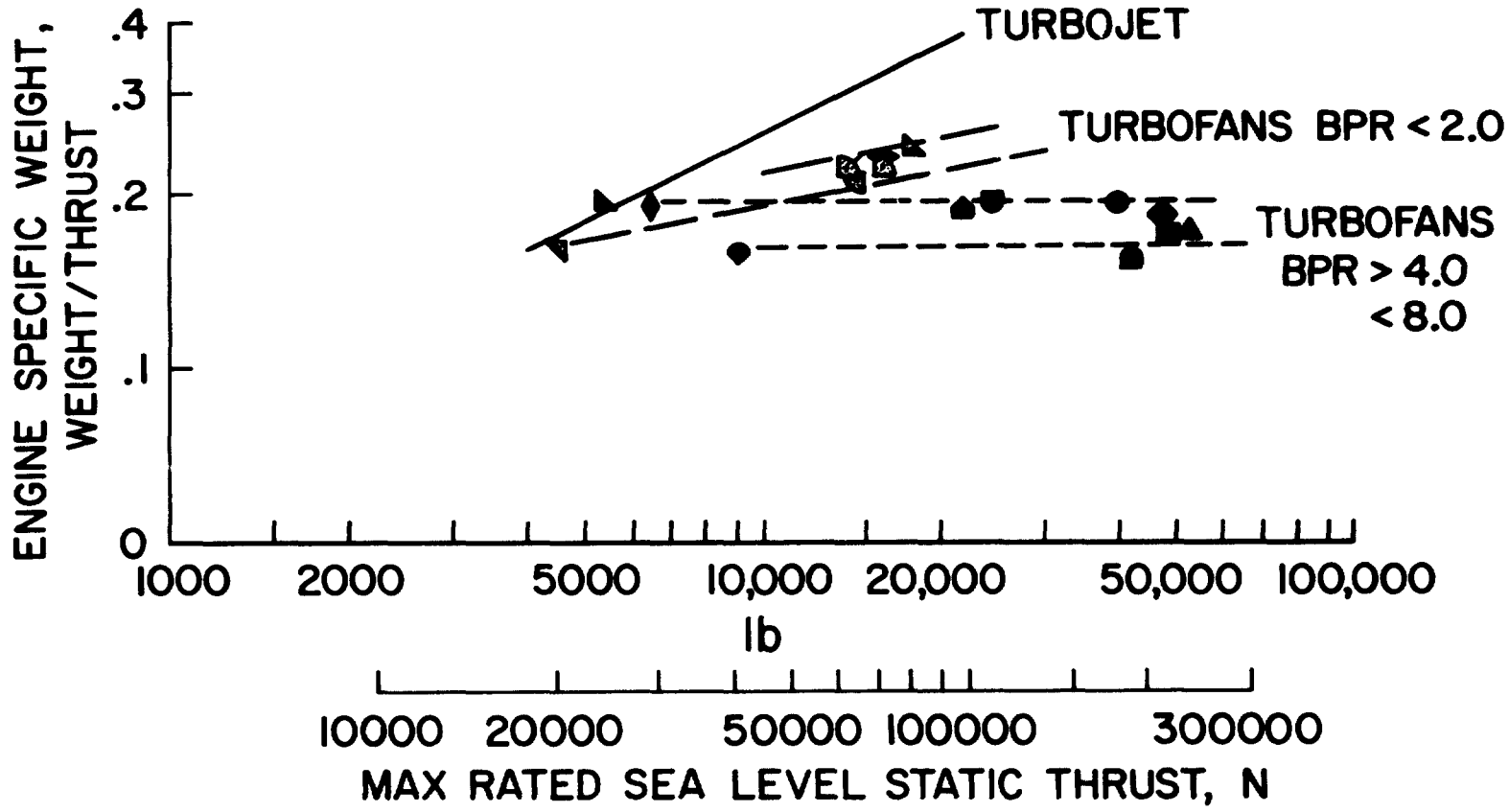

Figure 2.- Turbofan engine specific weights.

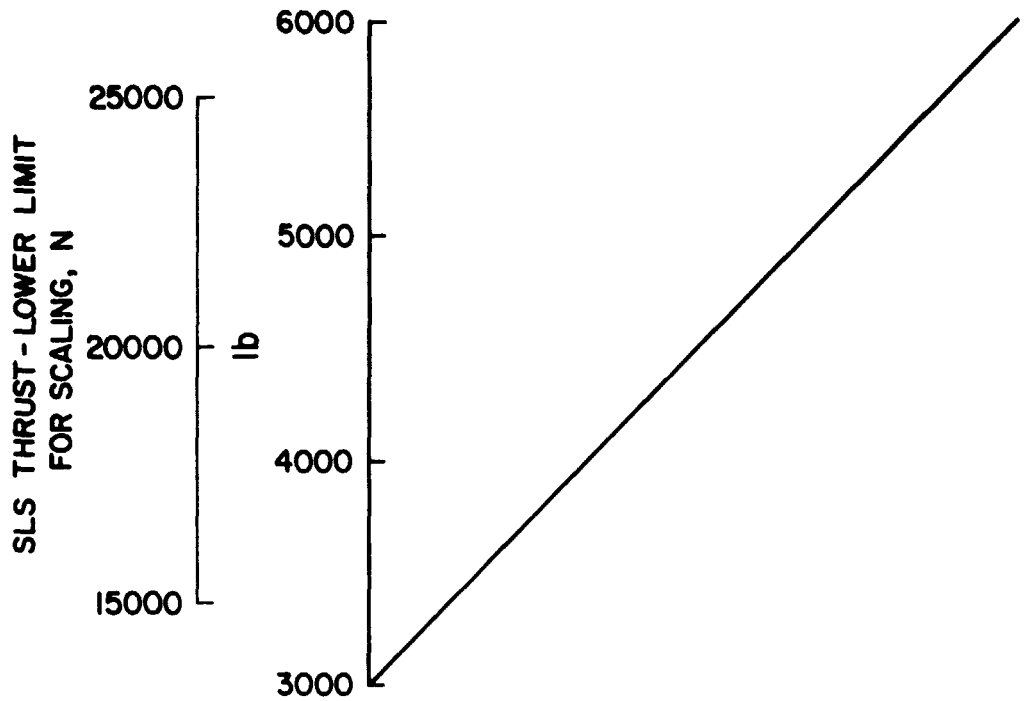

$$\frac{(\text{Sp wgt})_1}{(\text{Sp wgt})_2} = \left(\frac{T_1}{T_2}\right)^{\frac{n-2}{2}}$$

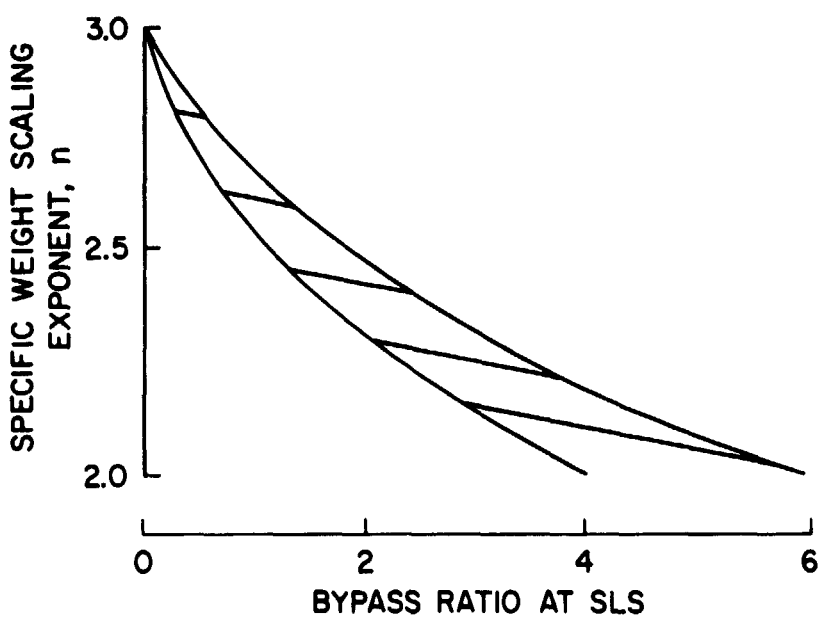

Figure 3.- Scaling exponents and thrust limits.

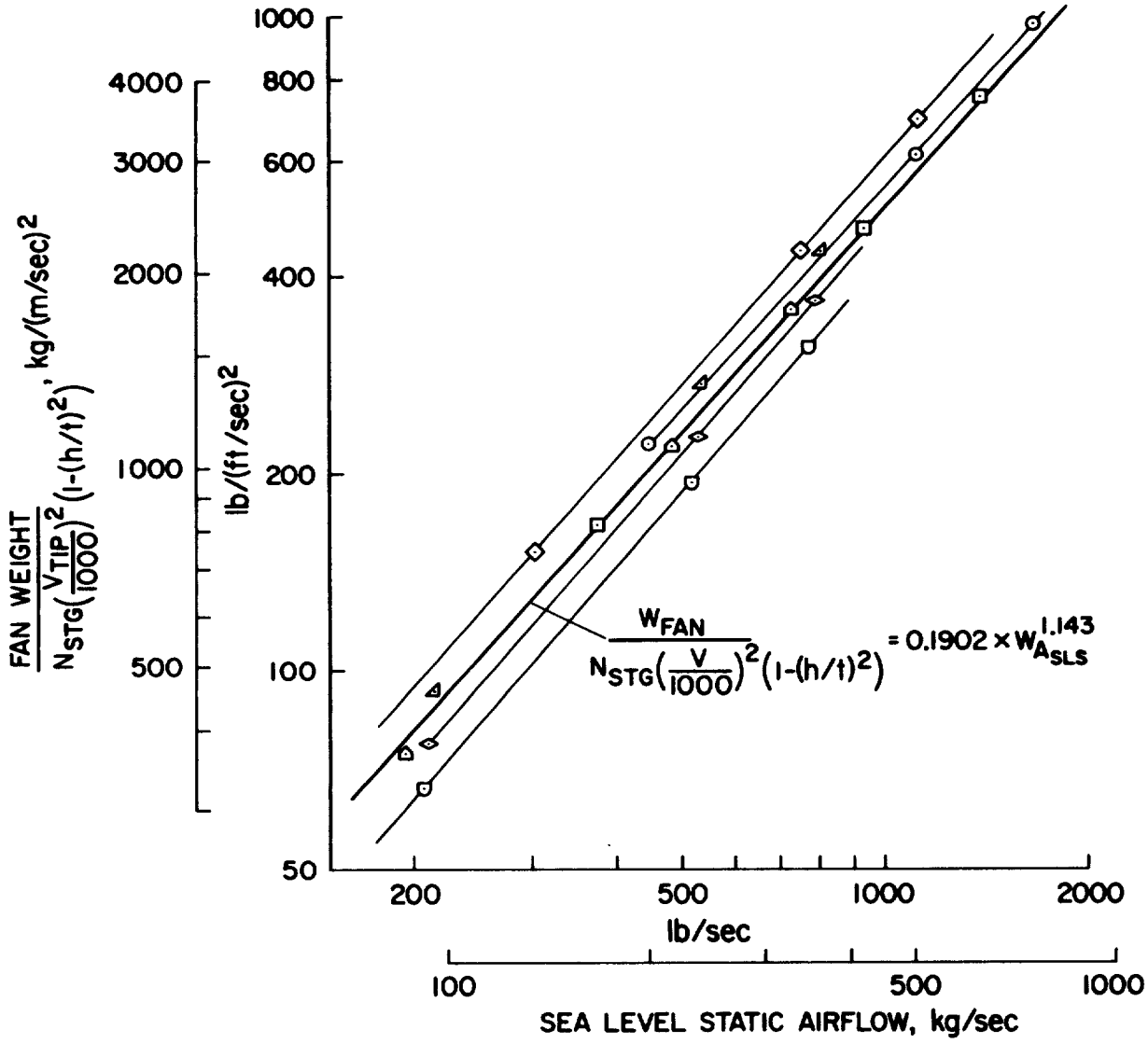

Figure 4.- Fan weights.

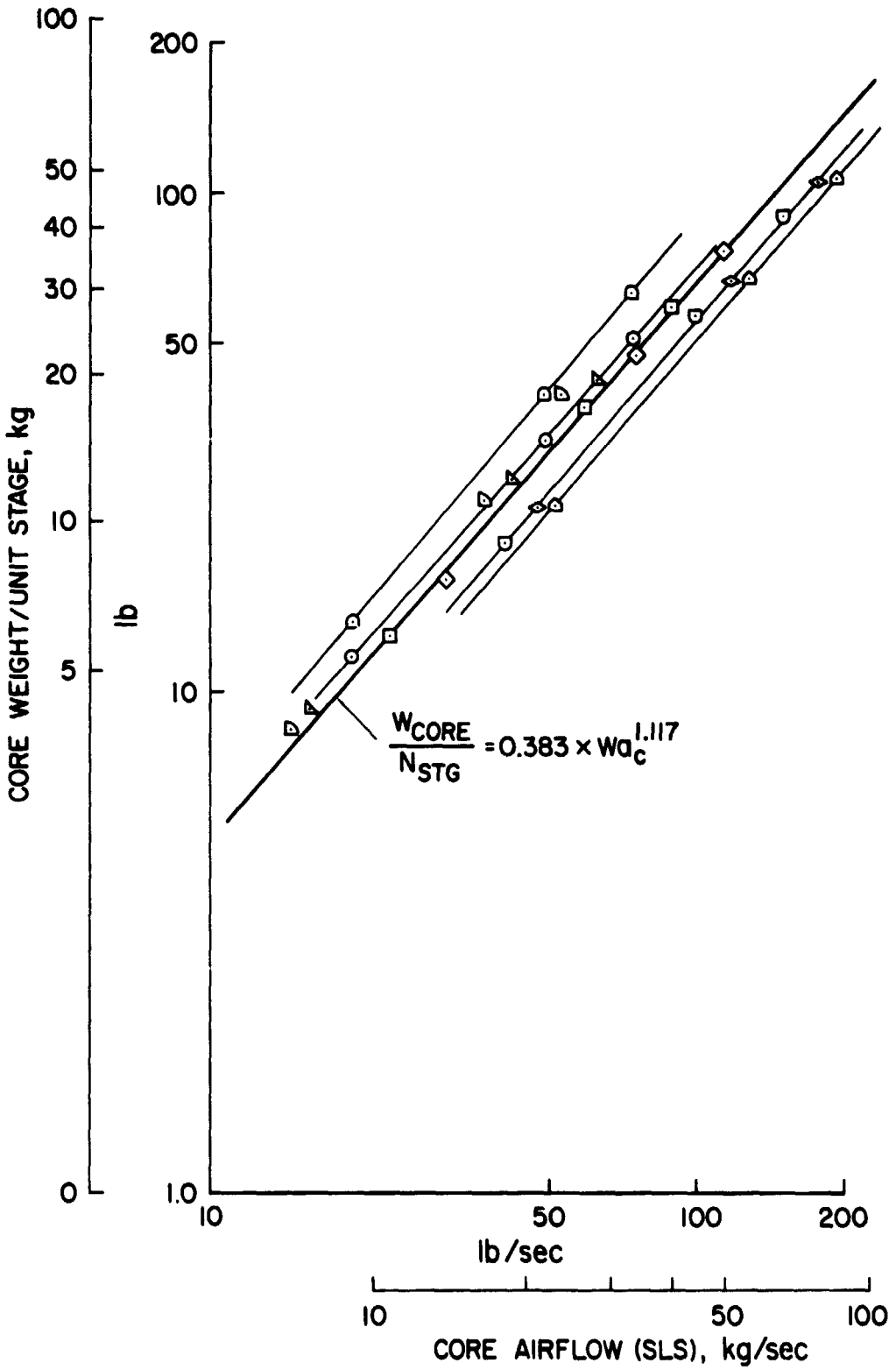

Figure 5.- Core engine weights.

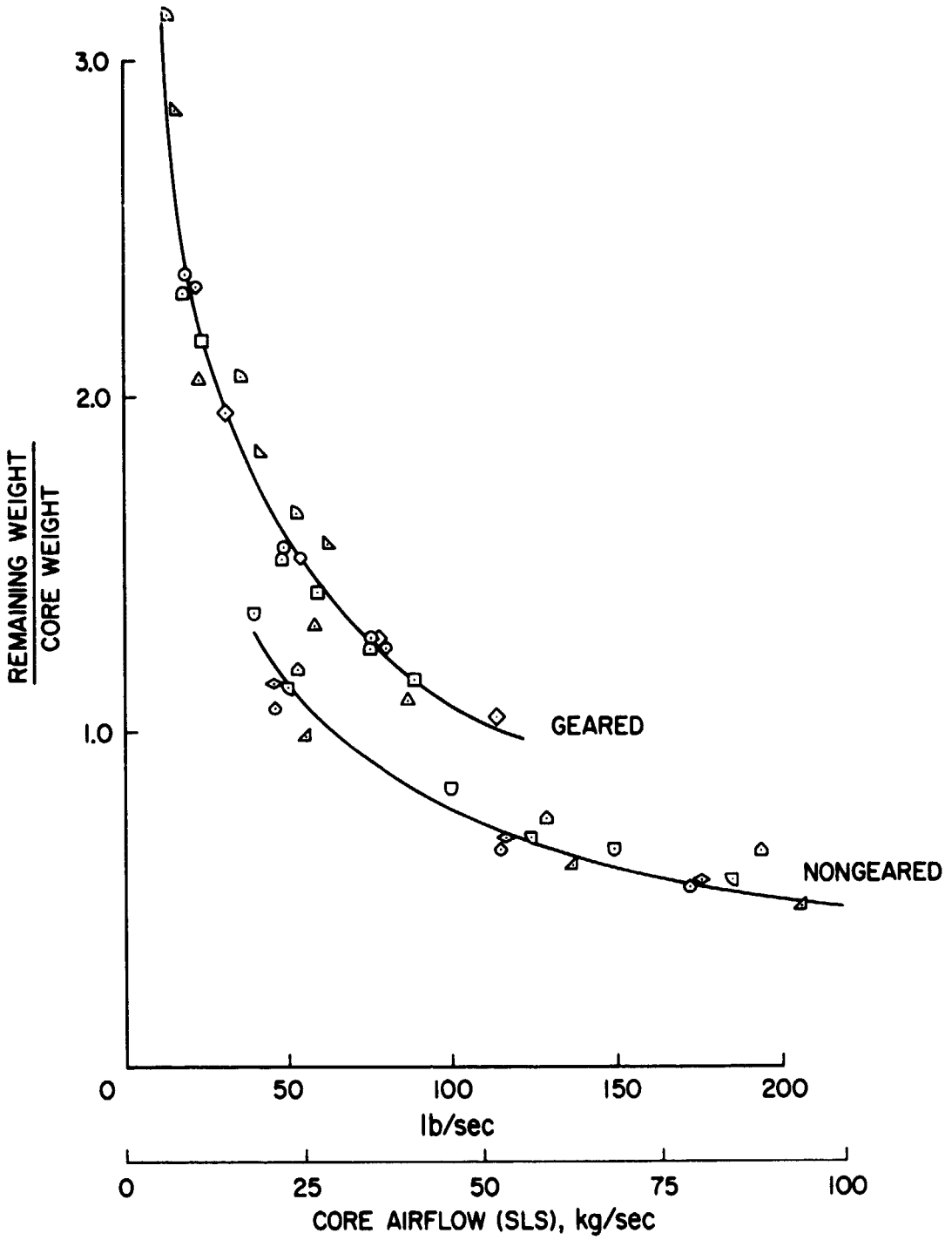

Figure 6.- Engine remaining weights.

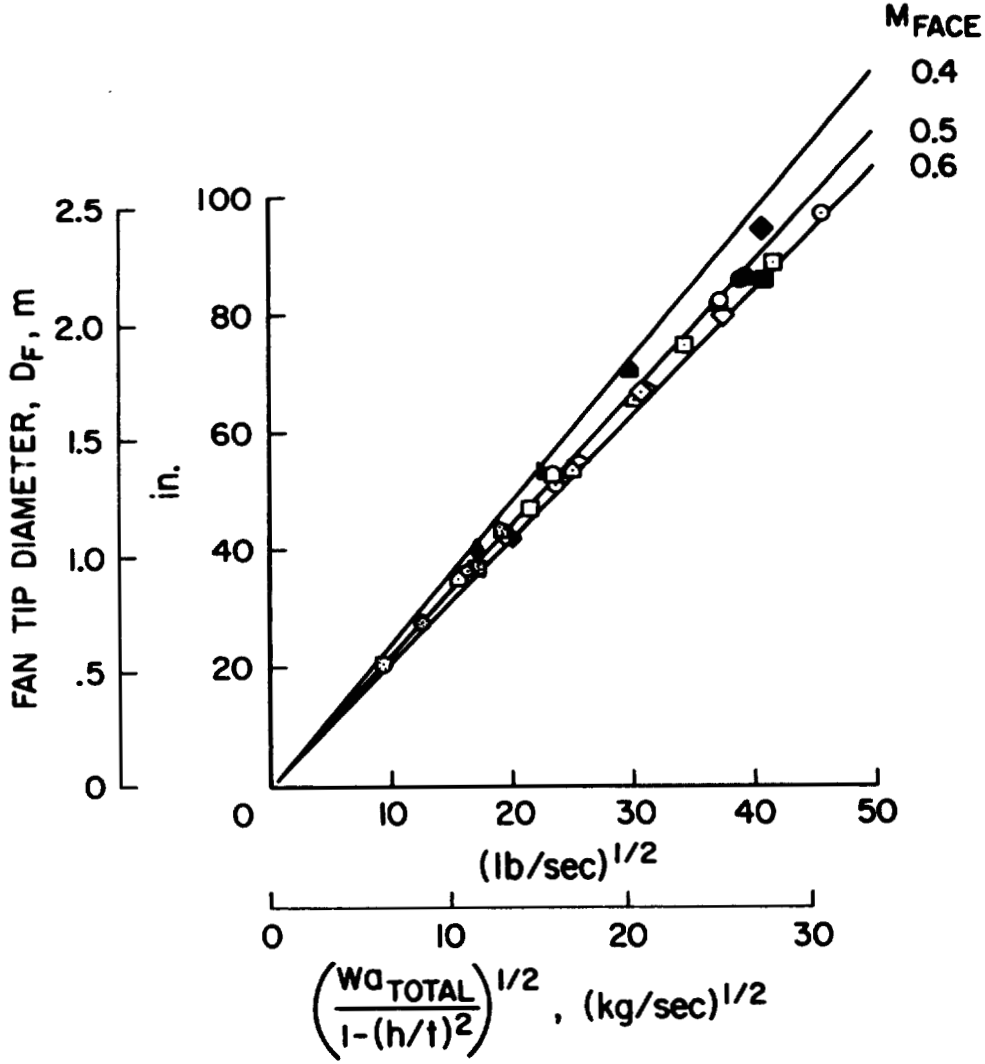

Figure 7.- Fan diameters.

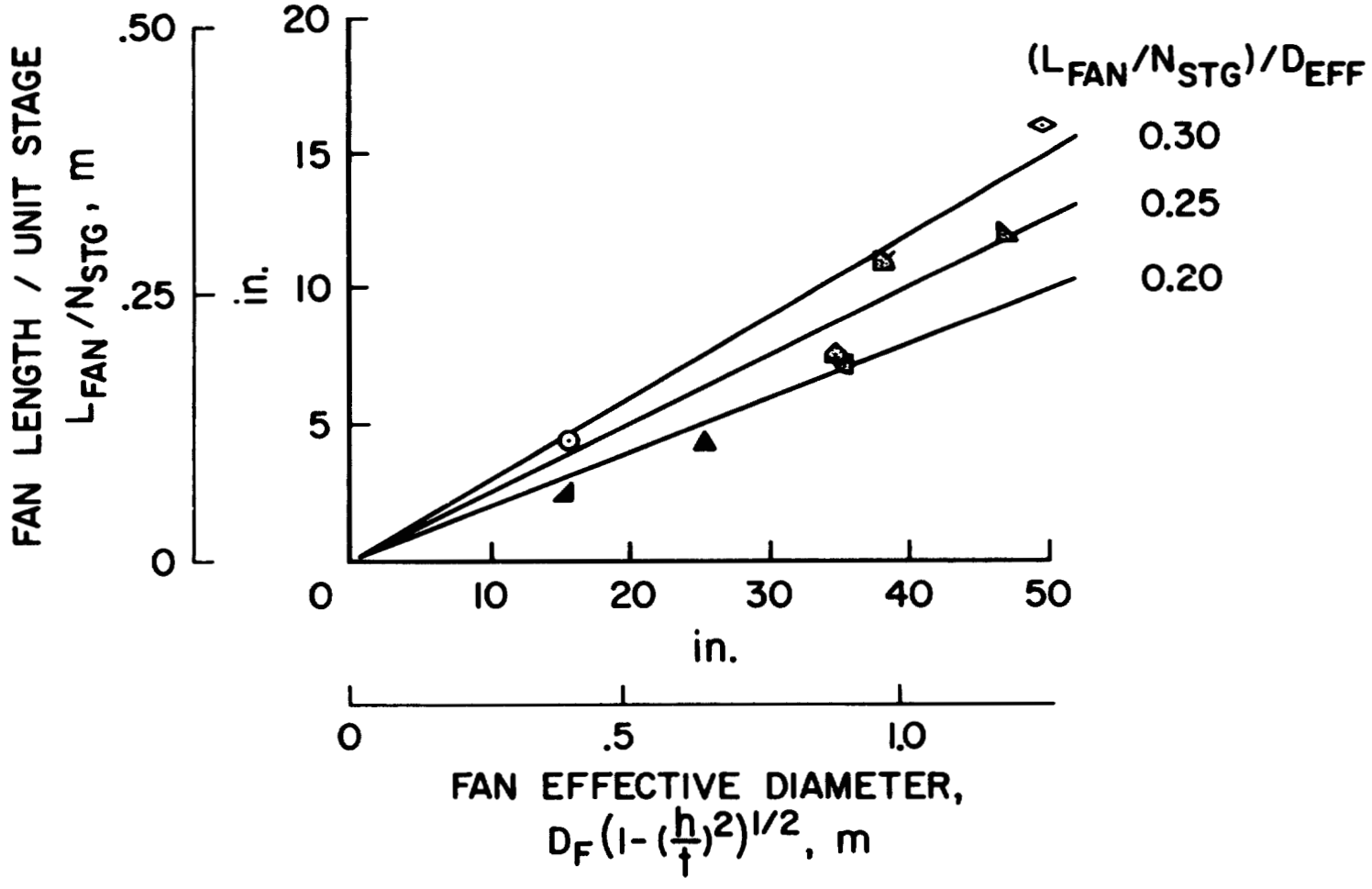

Figure 8.- Fan length per stage.

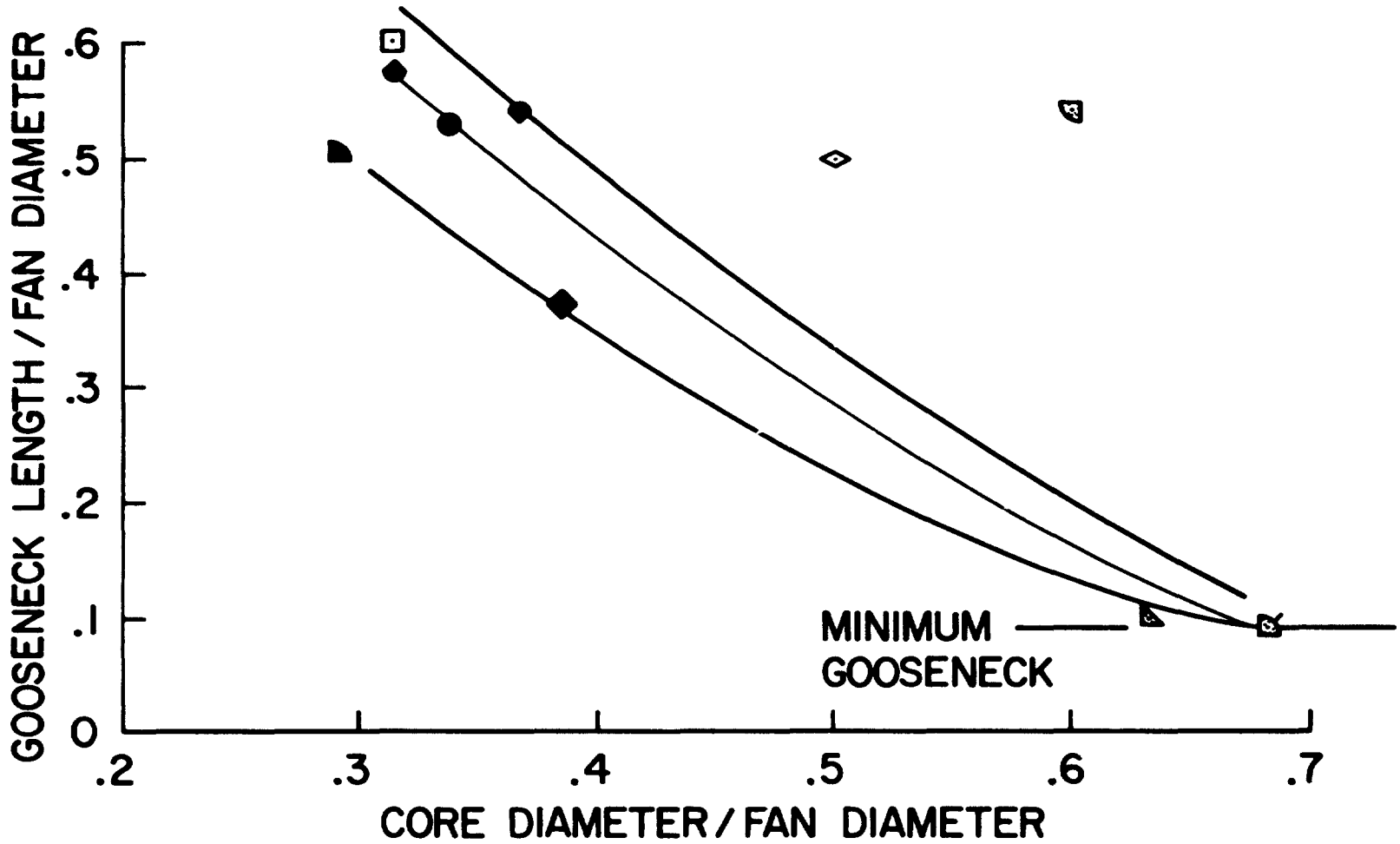

Figure 9.- Gooseneck lengths.

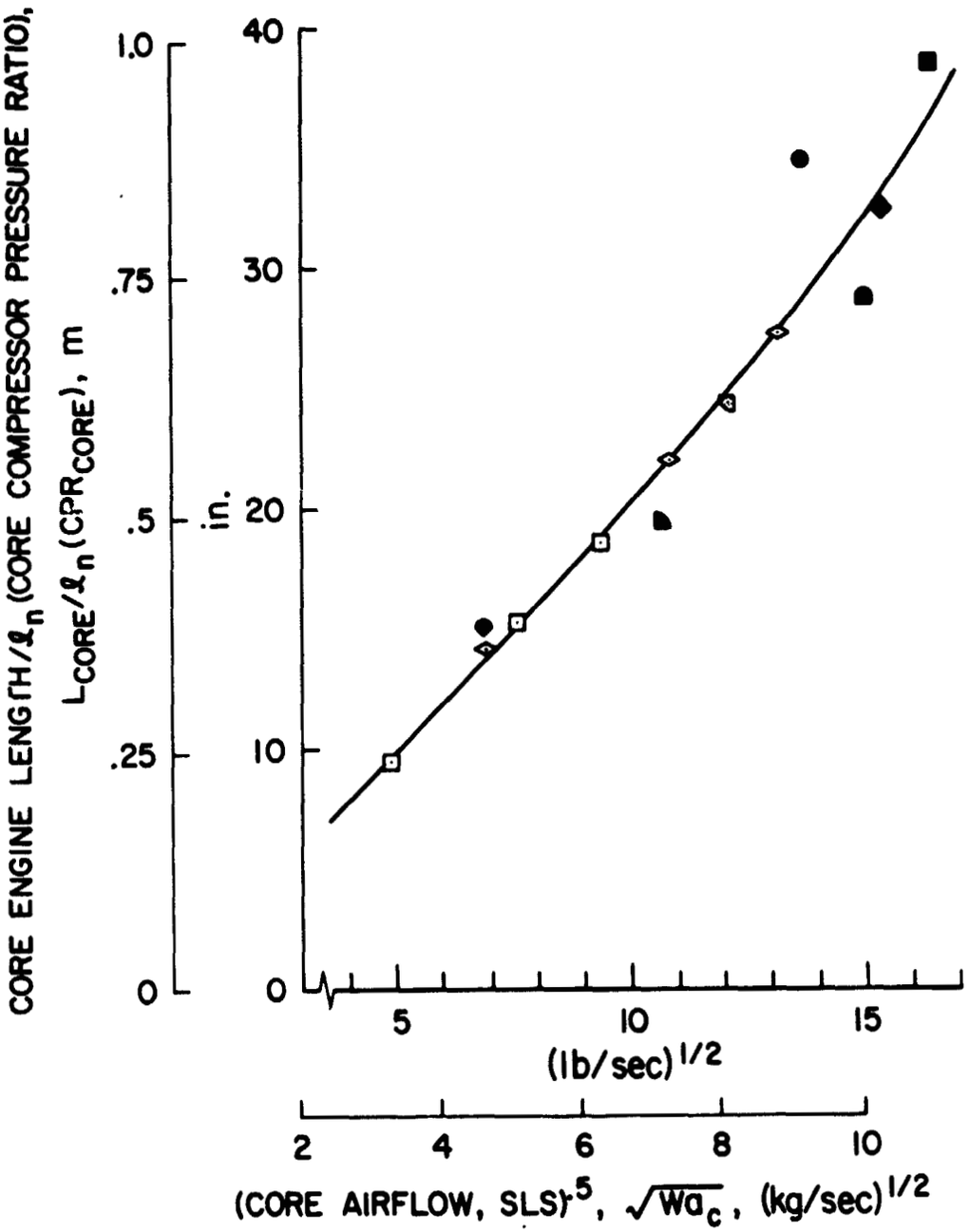

Figure 10.- Core engine lengths.

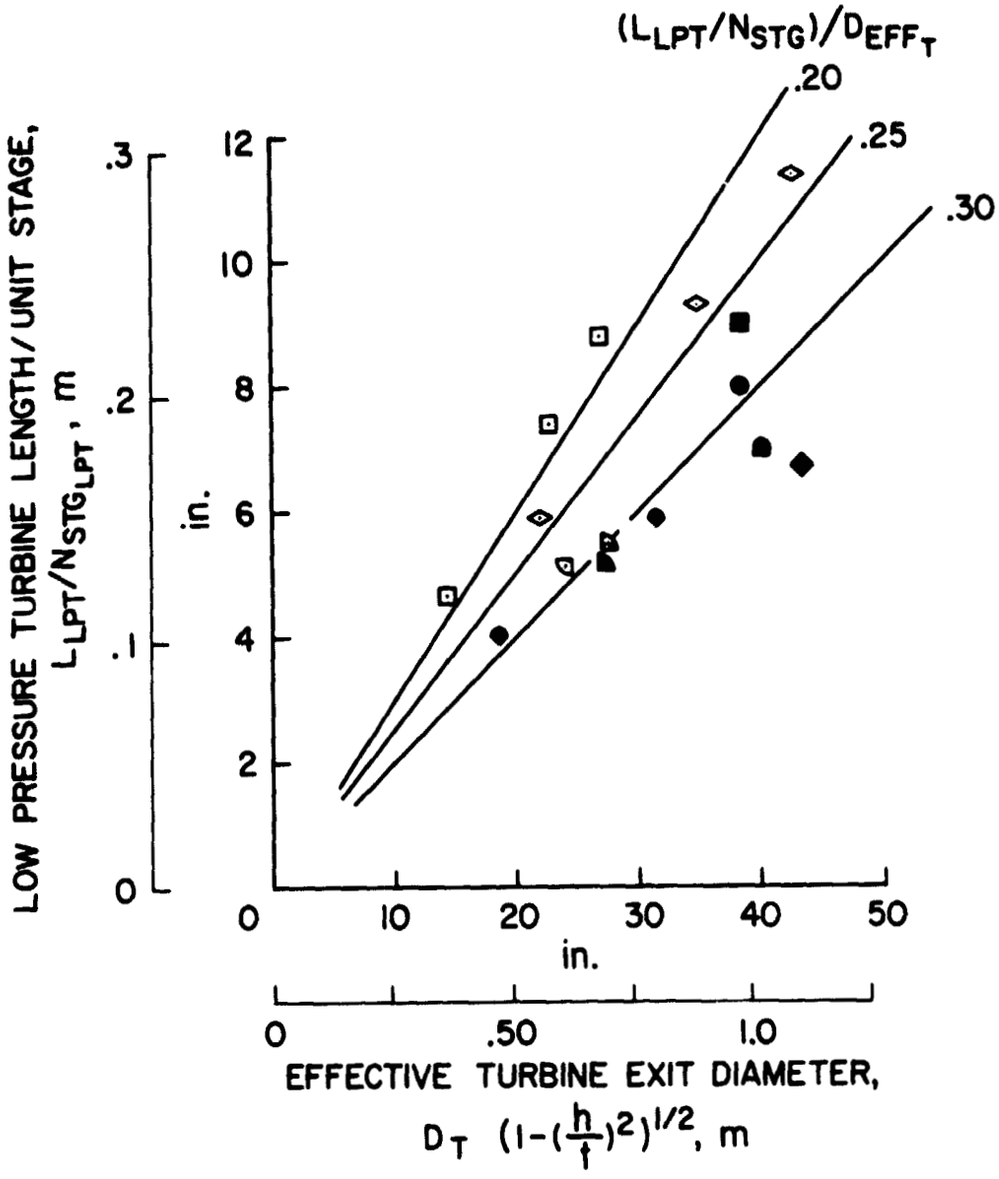

Figure 11.- Low-pressure turbine length per stage.

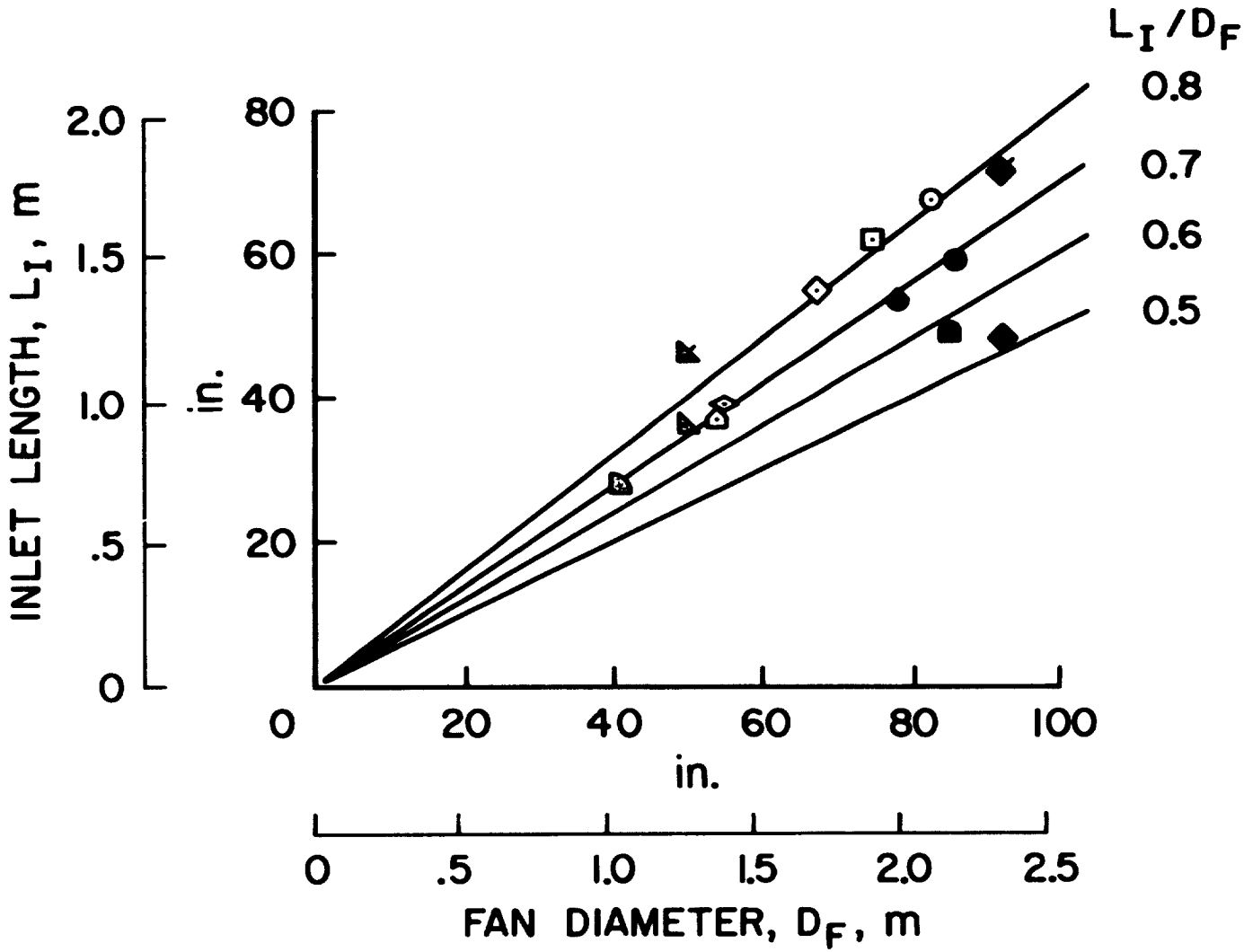

Figure 12.- Nacelle inlet lengths.

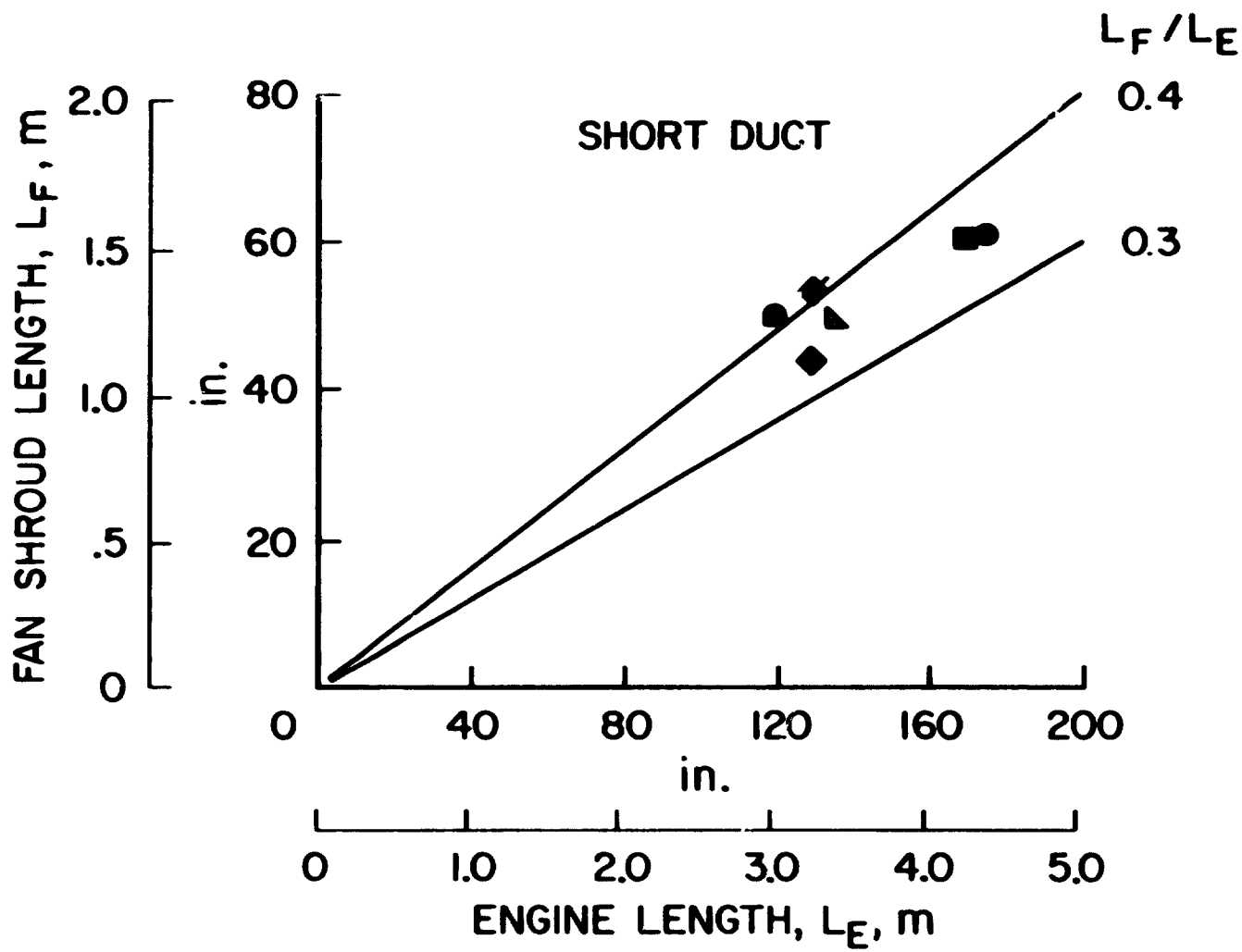

Figure 13.- Fan cowl lengths.

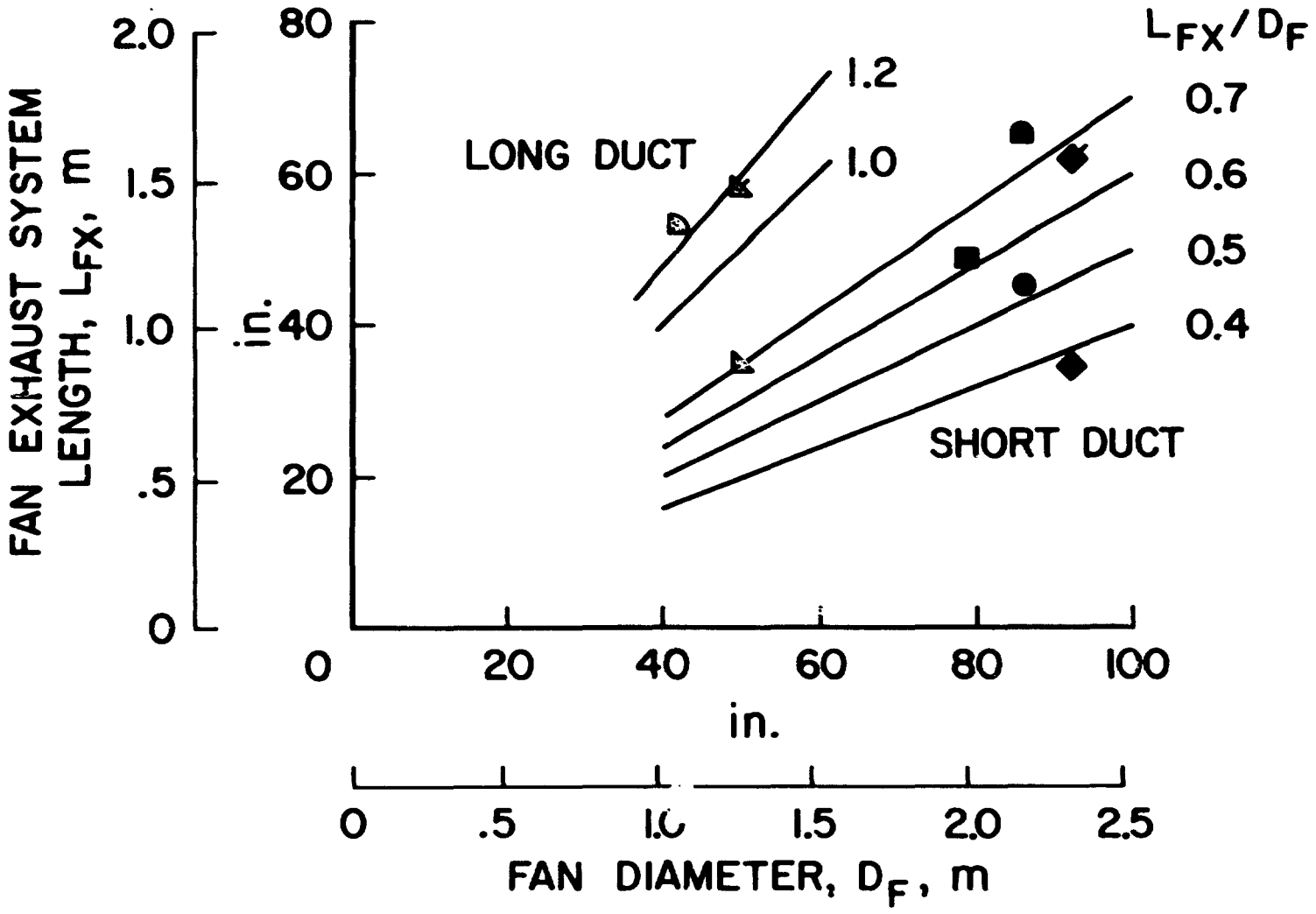

Figure 14.- Fan exhaust system lengths.

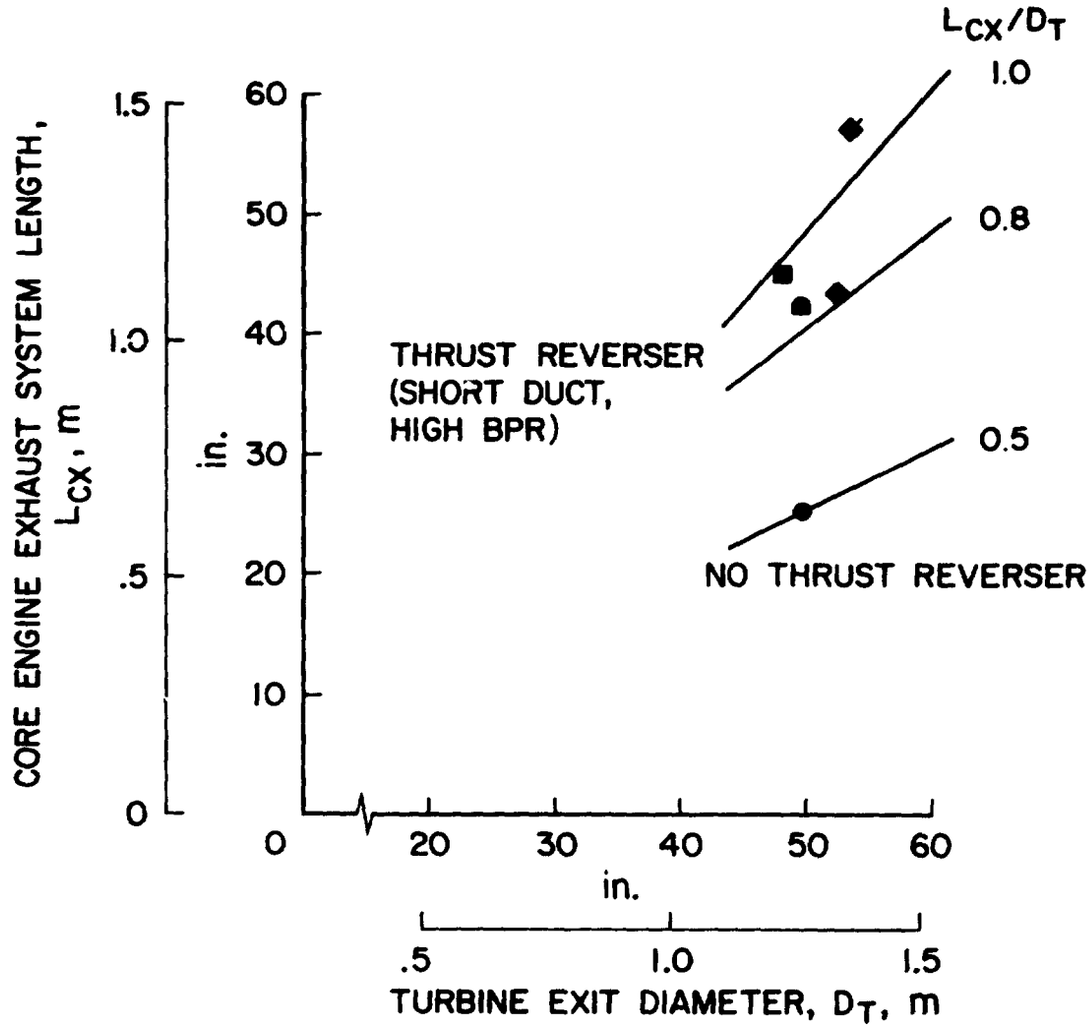

Figure 15.- Core exhaust system lengths.

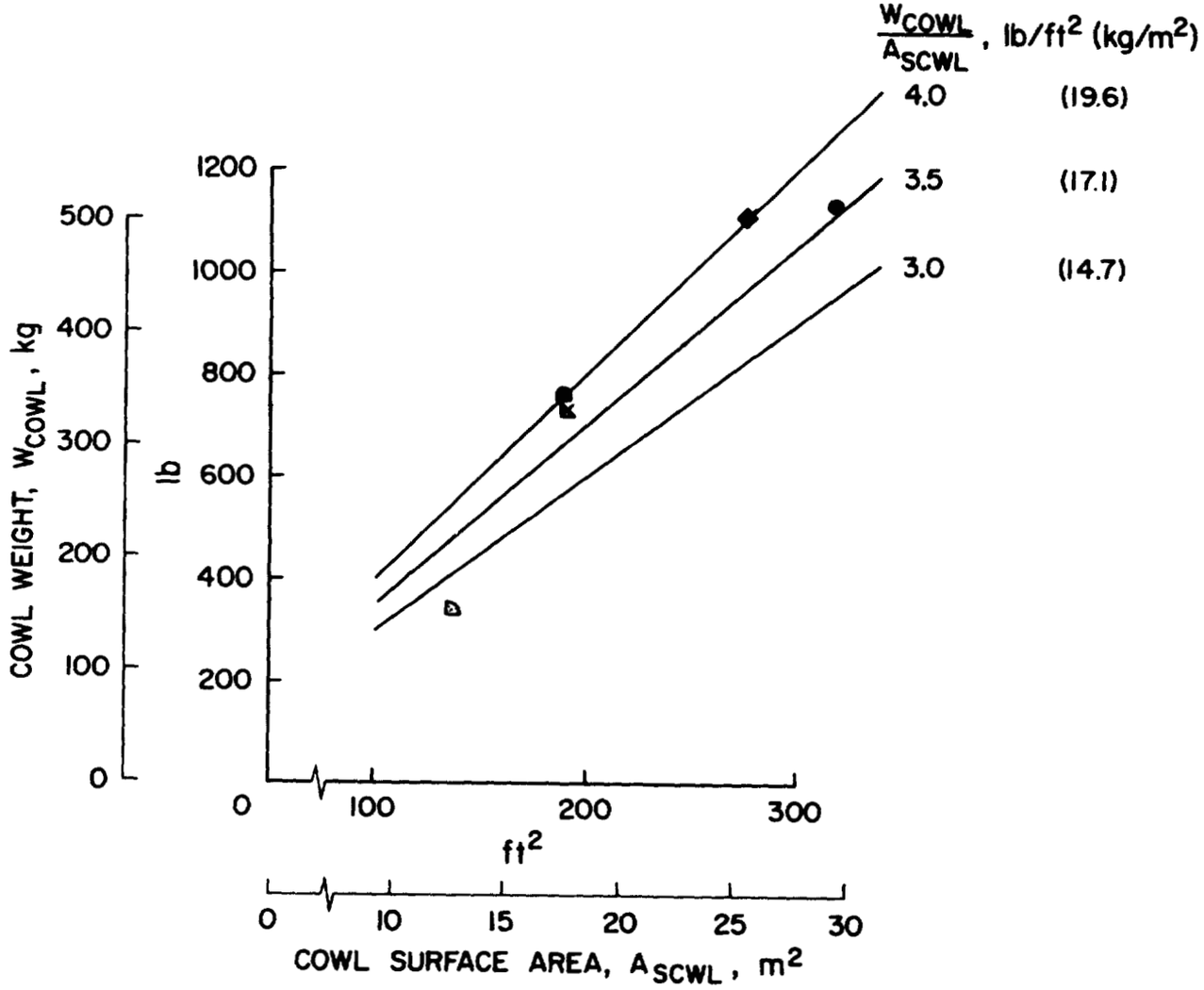

Figure 16.- Cowl weights.

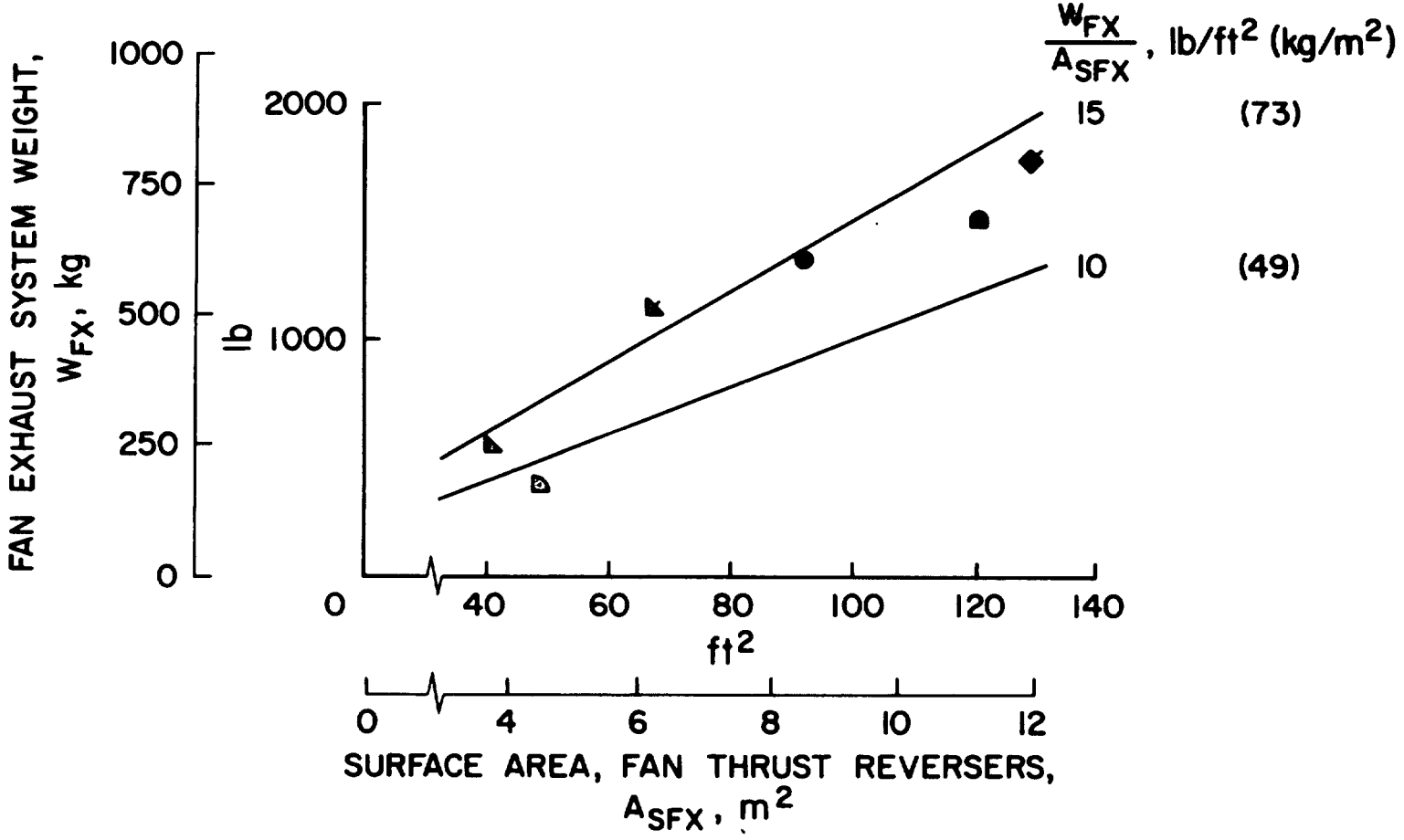

Figure 17.- Fan exhaust system weights.

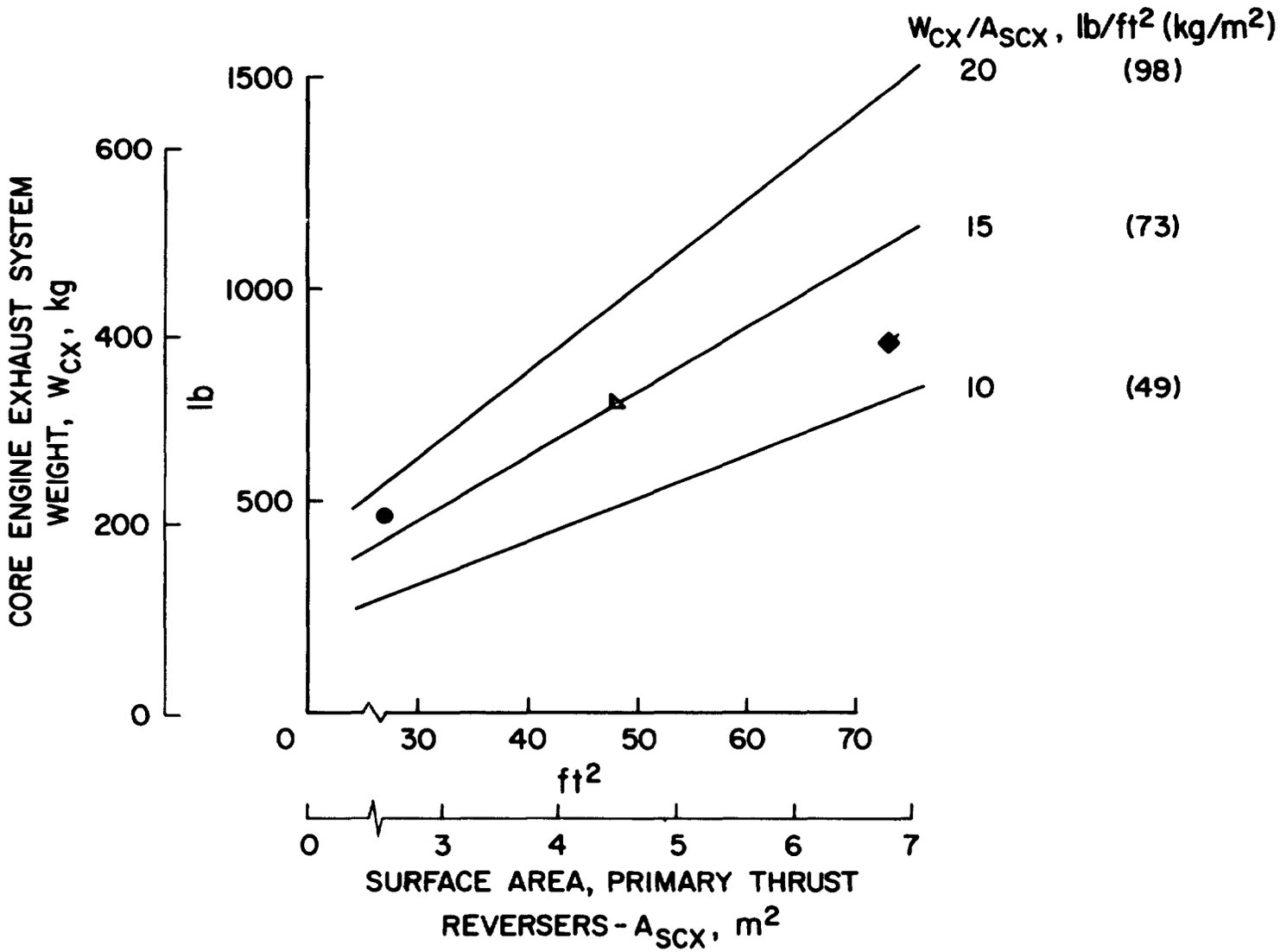

Figure 17.- Concluded.

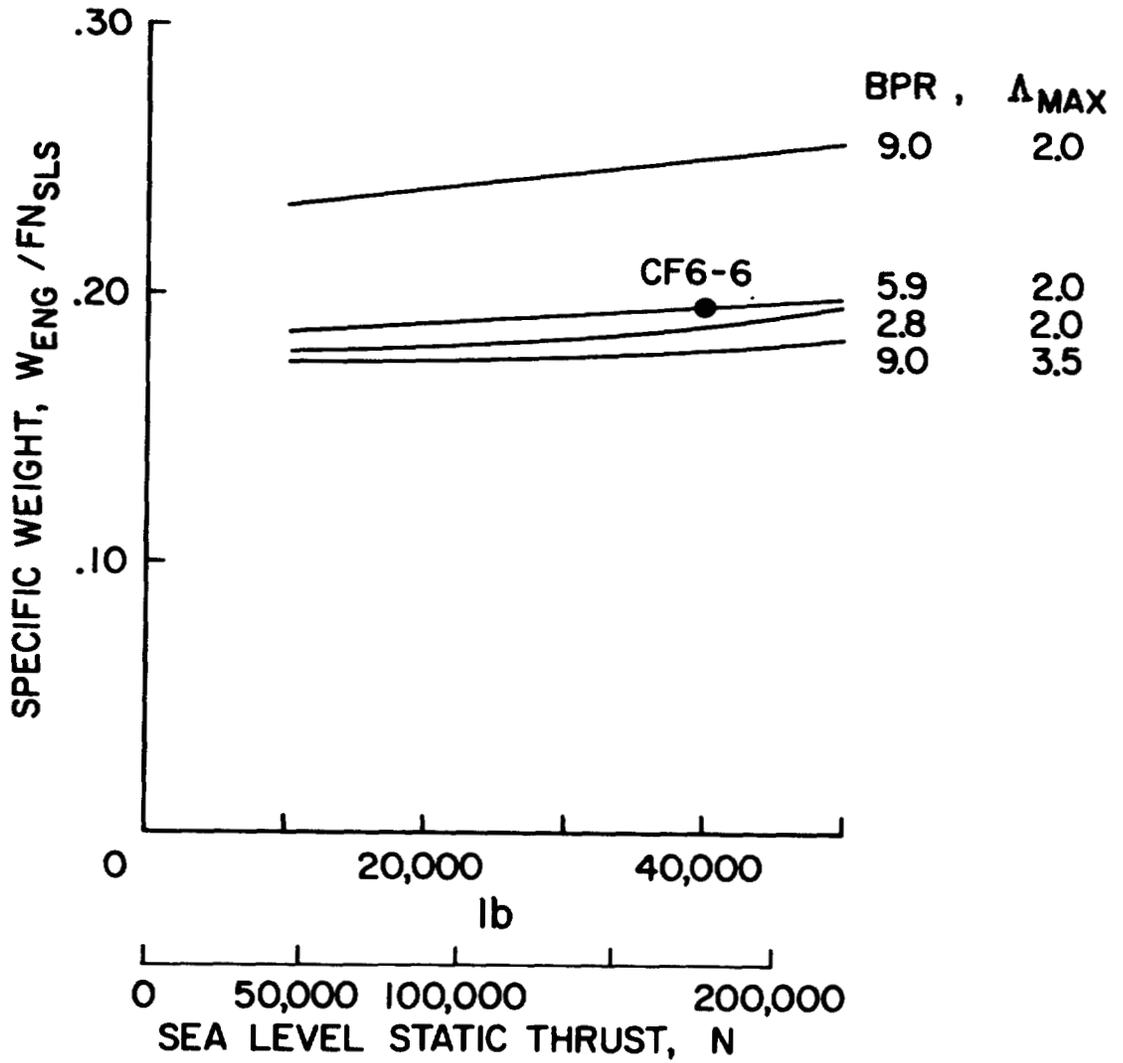

Figure 18.- Predicted engine specific weights.

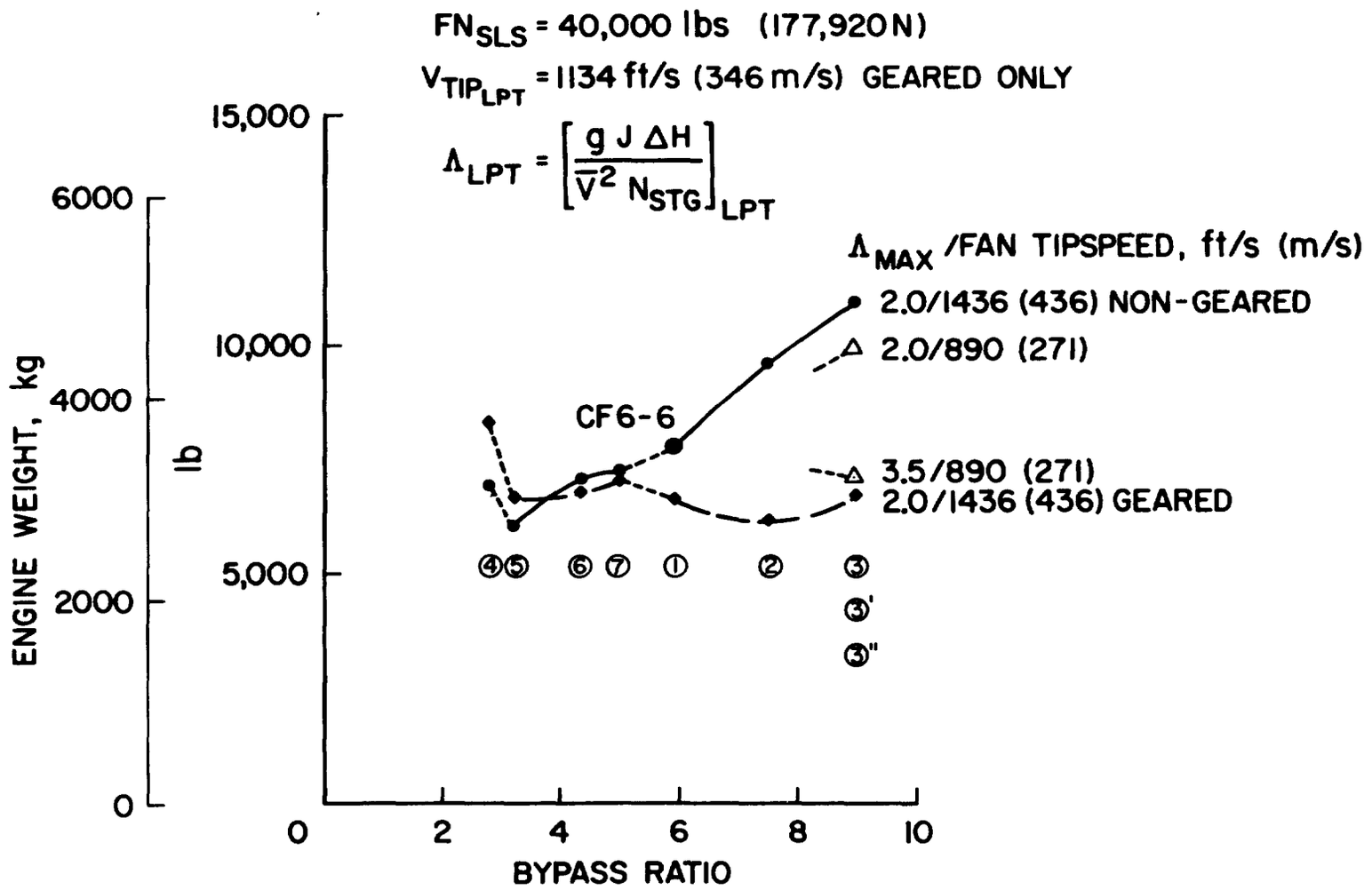

Figure 19.- Predicted engine weights: geared vs nongeared.

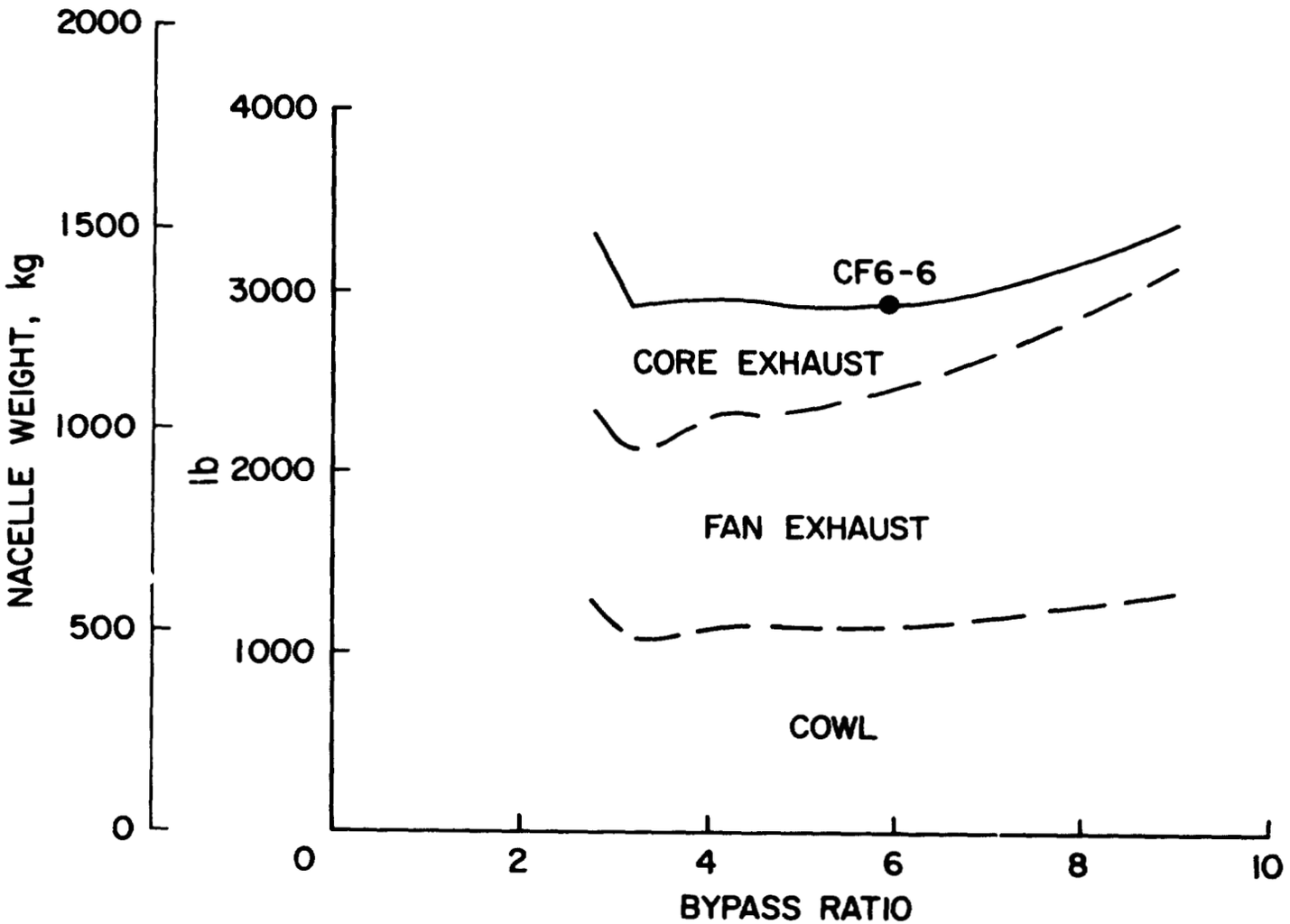

Figure 20.- Predicted nacelle weights.

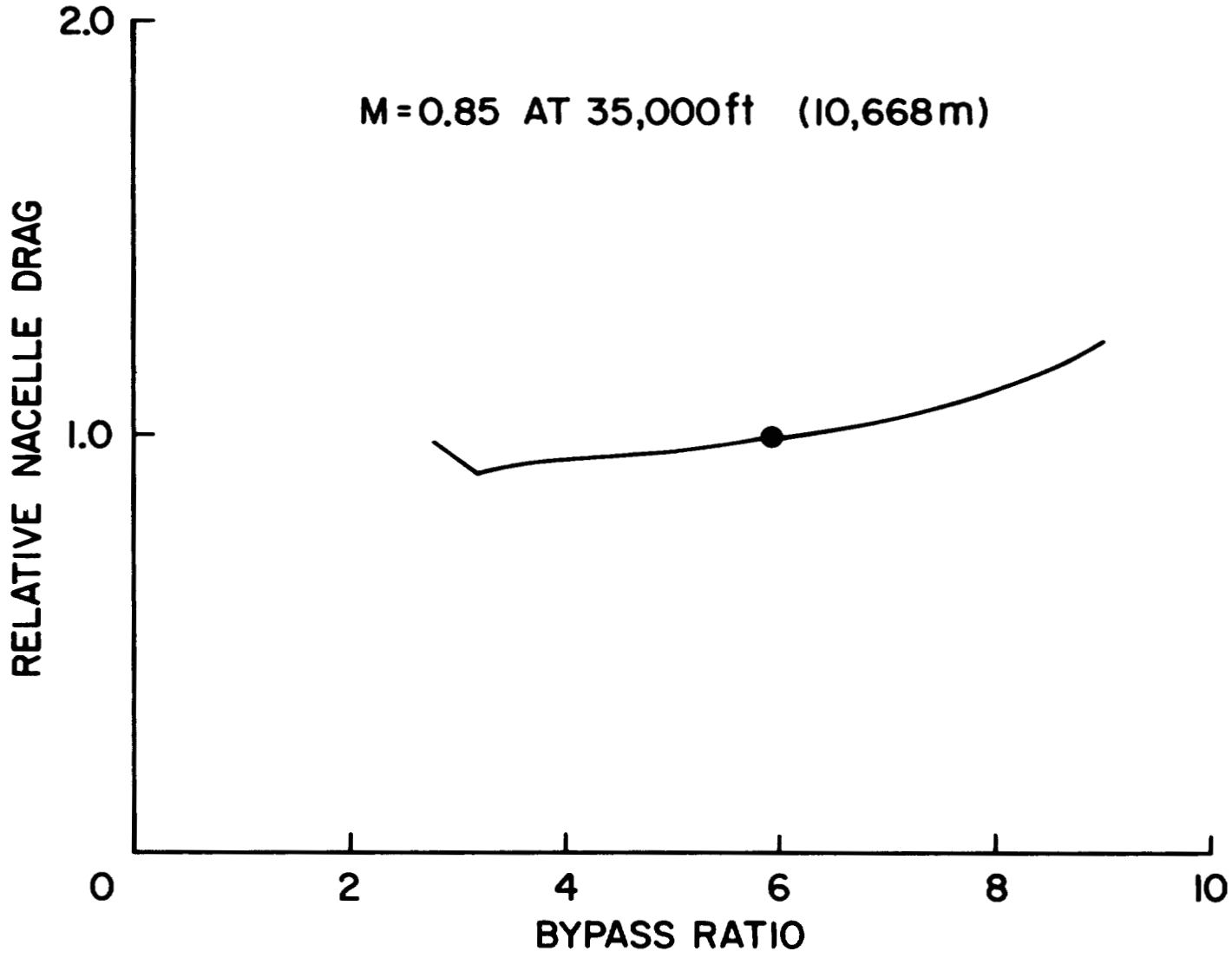

Figure 21.- Predicted nacelle drag.

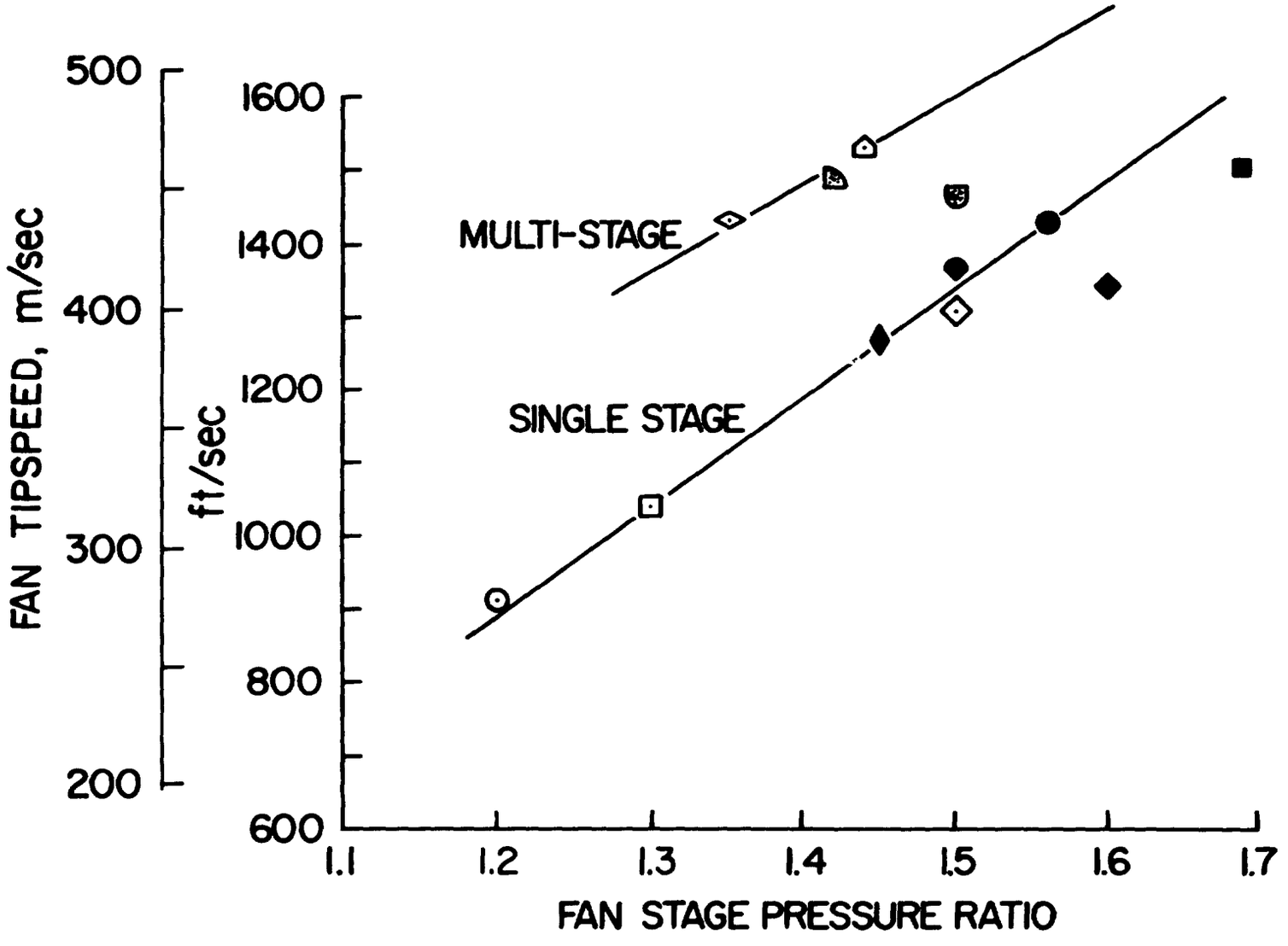

Figure 22.- Fan tipspeed correlation.

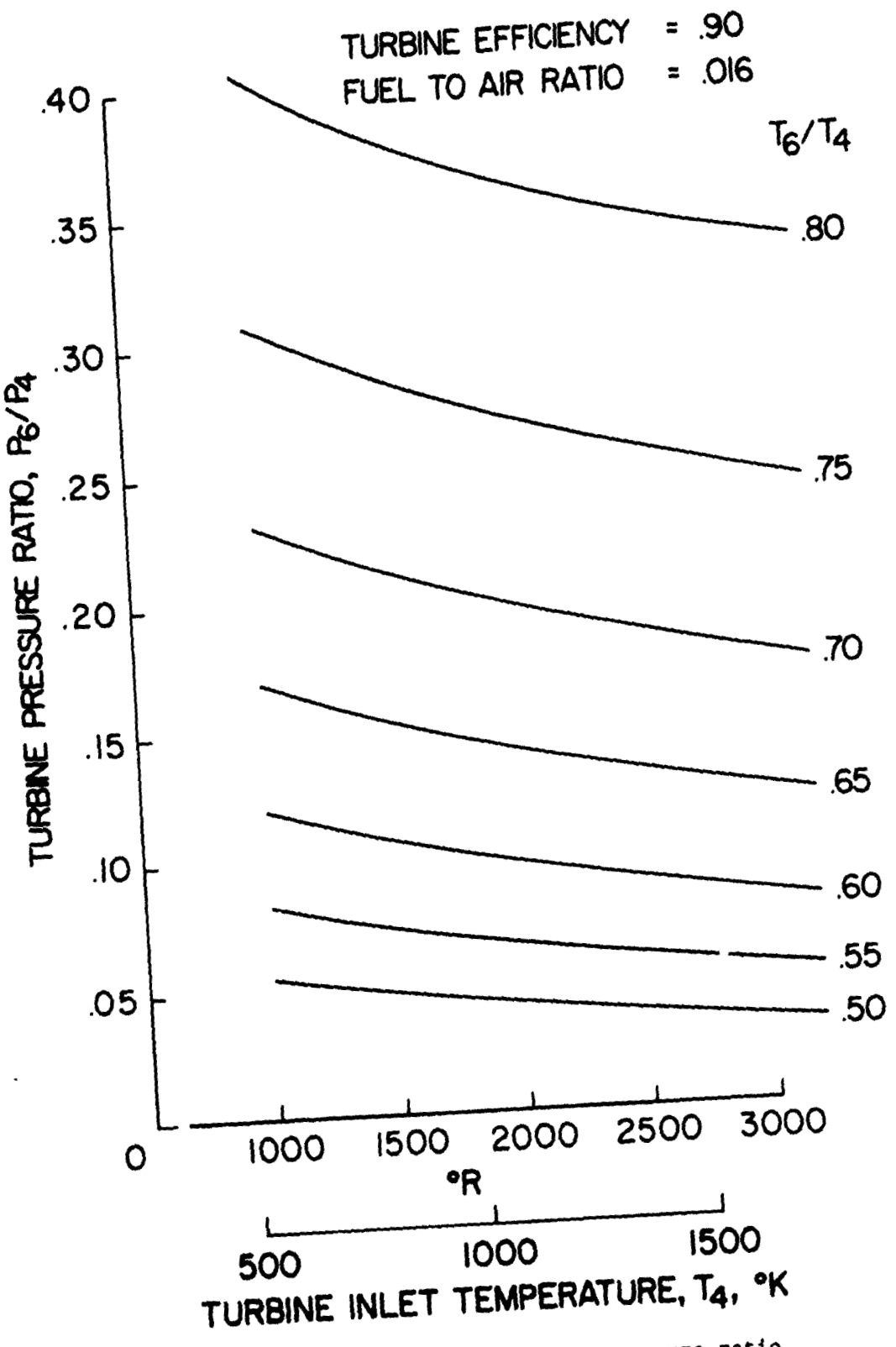

Figure 23.- Turbine pressure ratio.